UNITED NATIONS
UNIVERSITY

GEOTHERMAL TRAINING PROGRAMME
Orkustofnun, Grensasvegur 9,
IS-108 Reykjavik, Iceland

Reports 2012
Number 25

BOREHOLE GEOLOGY AND HYDROTHERMAL MINERALISATION OF WELL OW-911A, OLKARIA DOMES GEOTHERMAL FIELD, CENTRAL KENYA RIFT VALLEY

Doreen Wanjiku Njathi
Kenya Electricity Generating Company – KenGen
P.O. Box 785 – 20117
Naivasha
KENYA
dnjathi@kengen.co.ke; doreennjathi@gmail.com

ABSTRACT

Well OW-911A is a production well located in the Olkaria Domes, situated within the Greater Olkaria geothermal system. This directional well was drilled to a depth of 3006.3 m. Sampling of the cuttings was fairly good, except where circulation losses occurred at 78-222, 660-664, 720-722, 1742-1744, and at 2876-2886 m. The rock types encountered consist of pyroclastics, rhyolites, tuffs, trachytes and basalts. The top 78 m are made up of unconsolidated pyroclastics overlying the rhyolite, basalt, trachyte and tuff. At depth trachyte was found to dominate the lower part, intercalating with tuff and occasionally basalt. The first occurrence of crystalline epidote was at 670 m depth, indicating an alteration temperature of >240ºC below that depth. The well showed some permeability, as indicated by temperature logs, circulation losses and hydrothermal alteration mineralogy patterns. This report discusses the likely causes as to why OW-911A is a lower producer than the surrounding wells: OW-909, OW-908A, OW-910A and OW-912A. It also gives a subsurface view of the extent of the Domes since it appears to be located at the boundary of the Domes area.

1. INTRODUCTION

Well OW-911A is a directional well located in the southern section of the Domes area which belongs to the Olkaria Volcanic Complex in the central sector of the Kenya Rift (Figure 1). It is situated at 202736.34 Eastings and 9898315.71 Northings with an elevation of 1981.44 m and was aimed to strike the southwest fault structures of the Olkaria domes geothermal field (Figure 2). Its purpose was to be a production well but it turned out to be a poor producer, yielding only 1 MW. Well OW-911A was drilled to a depth of 3006.3 m with the surface, anchor and production casings set at 61.1, 305.5 and 951 m, respectively.

The main aim of this study was to determine the geothermal conditions in the Olkaria Domes system by understanding the lithology, hydrothermal mineralisation, the sequence of mineral deposition in the veins and vesicles, locations of aquifers, and the temperature of the reservoir in this well. This study tries to resolve why the well is a much lower producer compared to the surrounding wells, OW-909, OW-908A, OW-910A and OW-912A, and also to determine the subsurface extent of the Domes since the well's direction is southeast towards the boundary of the Domes area. This geological research is mostly based on available data from the time of drilling and subsequent laboratory analyses.

The geological setting of the well is described in Section 2, methodology is in Section 3, borehole geology in Section 4, hydrothermal alteration in Section 5, and Sections 6 and 7 include discussion and conclusions, respectively.

2. REGIONAL GEOLOGICAL SETTING AND TECTONICS

2.1 Geological setting

The Greater Olkaria geothermal area is situated south of Lake Naivasha on the floor of the southern segment of the Kenya rift. The Kenya rift is part of the East African rift system that runs from the Gulf of Eden in the north to Beira, Mozambique in the south. It is the segment of the eastern arm of the rift that extends from Lake Turkana in the north to Lake Natron, northern Tanzania, in the south (Figure 1). The rift is part of a continental divergent zone where spreading occurs, resulting in thinning of the crust, hence the eruption of lavas and associated volcanic activities (e.g. Lagat, 2004).

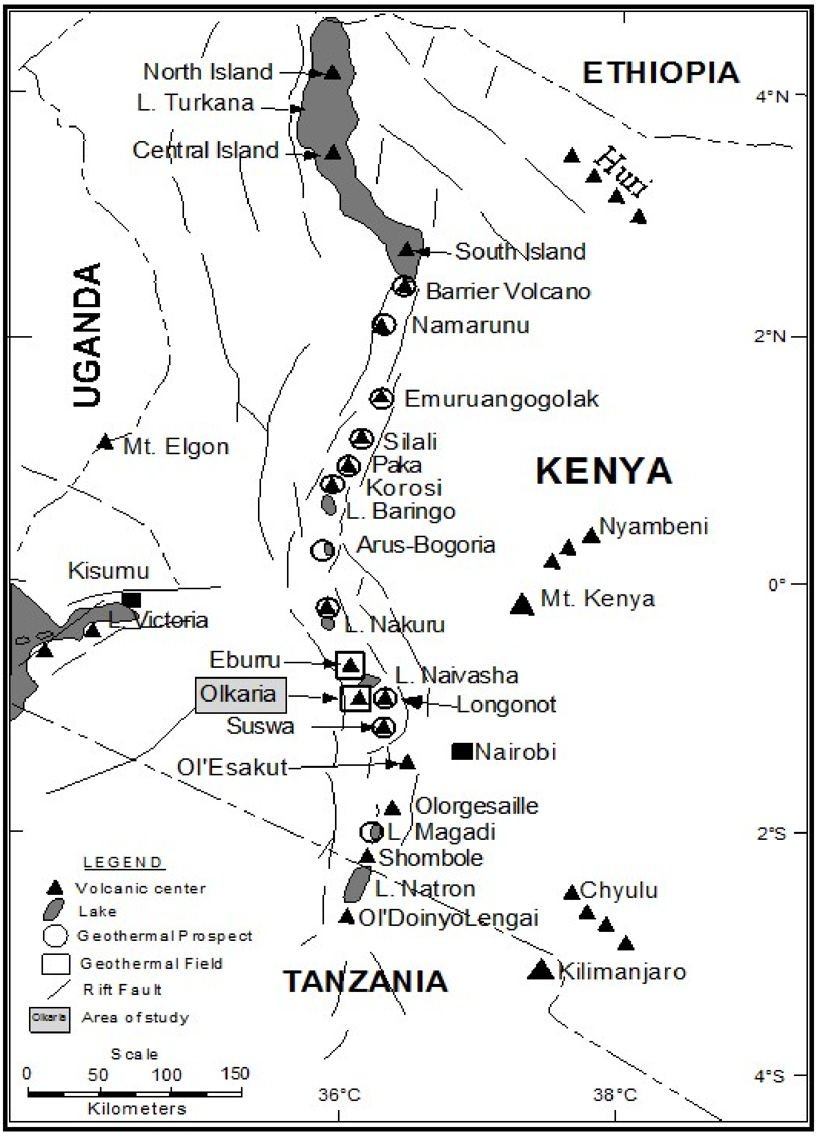

FIGURE 1: Map of the Kenya rift showing the location of Olkaria geothermal field and other Quaternary volcanoes along the rift axis (Lagat, 2004)

Surface mapping by Naylor (1972) identified the Olkaria area as being within an older caldera complex which was subsequently cut by N-S normal rift faulting that provided the loci for the rhyolitic dome eruptions now exposed east of Ol'Njorowa gorge (Figure 2). Later volcanic activity associated with the Olkaria volcano and the Ololbutot fault zone produced rhyolitic and obsidian flows, which were covered with pumice. Rhyolite domes form a circular pattern in the Domes area along a presumed caldera margin (Figure 2). Much of the area has subsequently been blanketed by a surface cover of young (Quaternary) pyroclastic deposits, believed to have originated primarily from the Longonot volcano and to a lesser extent Mt. Suswa (Mungania, 1999). Areas of altered and warm grounds are extensive throughout the Olkaria area and, together with the present surface manifestations, show a close association with the dominant N-S structures in the centre of Olkaria and the ENE-WSW oriented Olkaria fault zone (Figure 2).

2.2 The geoscientific aspect of the Olkaria field

The Greater Olkaria geothermal area (Figure 2) is within the Greater Olkaria volcanic complex. It is subdivided into seven fields for geothermal developmental purposes, namely Olkaria East, Olkaria Northeast, Olkaria Central, Olkaria Northwest, Olkaria South-west, Olkaria Southeast and Olkaria Domes (Figure 2).

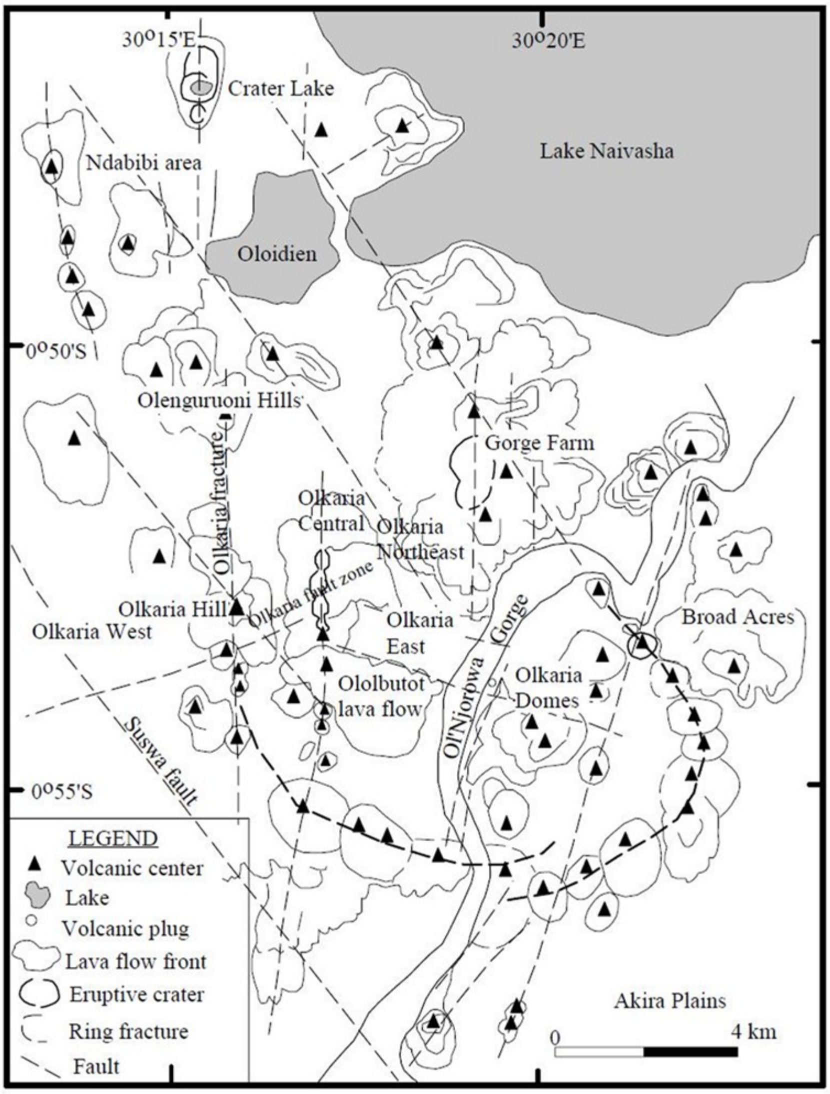

FIGURE 2: Volcano-tectonic map of the Greater Olkaria volcanic complex (Lagat, 2004)

The litho-stratigraphy of the Olkaria geothermal area, as revealed by data from geothermal wells and regional geology, can be divided into six main groups, namely: Proterozoic "basement" formations, Pre-Mau volcanics, Mau tuffs, plateau trachytes, Olkaria basalt and Upper Olkaria volcanics in chrono-stratigraphic order from the oldest to the youngest (Lagat, 2004). The drilled lithological column of OW-911A is composed of unconsolidated pyroclastics that occur at the shallowest levels overlying the rhyolite, basalt, trachyte and tuff. Trachyte is found to dominate the bottom of the well but it intercalates with tuff and occasionally basalt. This is typical of the Olkaria geothermal field (Omenda, 1998).

Geophysical analysis of resistivity anomalies at Greater Olkaria Geothermal area is based on transient electromagnetic (TEM), DC Schlumberger and magnetotelluric (MT) soundings. The results from these measurements indicate that the low resistivity anomalies are controlled by structural trends and that the geothermal resource is defined by a low resistivity of 15 Ωm (Furgerson, 1972; Mwangi, 1986; Dimitrios, 1989; Onacha, 1989, 1990 and 1993). Interpretation of gravity data indicates that a dense body occurs in the southern part of Olkaria between the Ol'Njorowa gorge and the Suswa lineament (Ndombi, 1981). The Olkaria West, Olkaria East and Olkaria Northeast fields occur within gravity lows. A gravity survey of the shallow crust beneath Olkaria indicates a volcanic zone of three layers that is down-faulted in the Olkaria West area. Dense dyke material of rhyolitic composition occurs along the Ololbutot fault, separating the western and eastern sectors of the Greater Olkaria geothermal area. This system of dykes is thought to be a significant hydrogeological barrier between the Olkaria West field, on one hand, and the Olkaria East and Olkaria Northeast fields, on the other (Lagat, 2004).

Seismic monitoring indicates that the area is characterised by a relatively high level of micro-earthquake activity. An analysis of focal depth, event location and classification shows that high frequency events and deep low frequency events occur at the intersection of structures in the area. The Olkaria Central field shows seismicity characterised by deep larger magnitude events. This implies that the area is active but with a deeper brittle-ductile zone. This has been interpreted to indicate that the area is not close to a strong heat source but rather that it is cooling by cold inflow (Simiyu et al., 1997, 2000). Seismicity shows the Olkaria Domes area to be a continuation of the Olkaria Northeast field along a major NW-SE linear structure. This area is characterised by both shallow and deep events that have been interpreted as volcano-tectonic and tectonic events (Simiyu et al., 1997). The area along the proposed southern ring fracture and the Ol´Njorowa gorge (Figure 2) is characterised by high frequency shallow events, which are interpreted as being related to shallow lateral fluid movement and may, therefore, not have high geothermal potential (Simiyu et al., 1997). Residual aeromagnetic data acquired within the Rift Valley show that the Olkaria area has a positive anomaly which has a NW-SE trend. The negative anomalies correspond to normally magnetised rocks, whereas the positive anomaly occurs in a demagnetised zone corresponding to the heat source that is of silicic origin. This provides some evidence for a heat source at a temperature above the Curie point of magnetite (above 575°C) close to the surface (Onacha, 1990). The occurrence of magnetic and gravity anomalies at the intersections of northeast and northwest rift faults is an indication of distinct near surface heat sources controlling the reservoir characteristics of the geothermal system (Lagat, 2004).

The fluid chemistry of the Olkaria West field contrasts sharply with that in the Olkaria East and Olkaria Northeast fields (Lagat, 2004). In the Olkaria West field, the discharge is typically rich in bicarbonates (10,000 ppm) but the Cl^- content is very low (50-200 ppm). Comparatively, the bicarbonates-carbonate and Cl^- content of the Olkaria Northeast field wells are <1000 ppm and 400-600 ppm, respectively. The Olkaria East fluid discharges have similar bicarbonates-carbonate concentrations of <200 ppm as in the Olkaria Northeast, and relatively low deep reservoir Cl^- concentrations of 200-350 ppm compared to Olkaria Northeast concentrations. Olkaria Central wells have deep reservoir Cl^- concentrations of 200-300 ppm, except for well OW-201, which has higher values in the order of 700 ppm. These wells produce waters with relatively high reservoir CO_2 concentrations, similar to those of the Olkaria West field wells. Olkaria Domes wells discharge mixed sodium bicarbonate-chloride-sulphate type water with low mean chloride concentrations of 181.5-269.9 ppm (Lagat, 2004).

3. SAMPLING METHODS AND ANALYSIS

3.1 Sampling

Samples of rock cuttings are taken at every 2 m interval during drilling but, in cases where the sample is too small and unrepresentative, up to a 4 m depth interval is sampled. Preliminary analysis is done at the rig site using a binocular microscope. During drilling, this acts as a guide for drillers denoting the hardness of the formations in order to avoid collapse of the formations, sticking of the drill strings and rapid wearing of bits. The samples are analysed further in the laboratory to provide a pictorial view of the subsurface and allow us to update the conceptual model of the geothermal system.

3.2 Analytical methods

Binocular microscope analyses of the cuttings samples are done by putting a sample into a petri dish and washing it with clean water to remove impurities and dust. The petri dish is filled with water to enhance visibility of the minerals and hidden features. A binocular microscope is used to note the colour(s) of the cuttings, rock type, grain size, texture, primary mineralogy, vein fillings, alteration mineralogy and intensity. Diluted hydrochloric acid is used to determine the presence of calcite.

The petrographic microscope is used to confirm the rock type and the alteration minerals, additional alteration minerals not observed by the binocular microscope, and to study the mineral depositional sequence of the alteration minerals.

XRD analysis is considered the best way to analyse hydrothermal clays. The clays can be used to determine alteration zone boundaries, especially at shallow depth. The clays can also be used to deduce the mineralogical sequence and as geothermometers.

Fluid inclusion analysis involves the analysis of trapped fluids inside mineral grains. A fluid inclusion is heated up until the gas bubble disappears and the temperature of homogenisation (Th) is measured. This is usually close to the temperature at which the fluid was trapped. It indicates the temperature of the system at that time.

4. BOREHOLE GEOLOGY

4.1 Drilling of well OW-911A

Well OW-911A is a directional well with a total drilled depth of 3006.26 m and is located at 202736.34 Easting and 9898315.71 Northing with an elevation of 1981.44 m above sea level. The well was drilled as a production well in the Olkaria Domes area (Figure 3), but its production was lower than what was expected compared to the surrounding wells. Drilling was aimed to strike the NE-SW striking structures

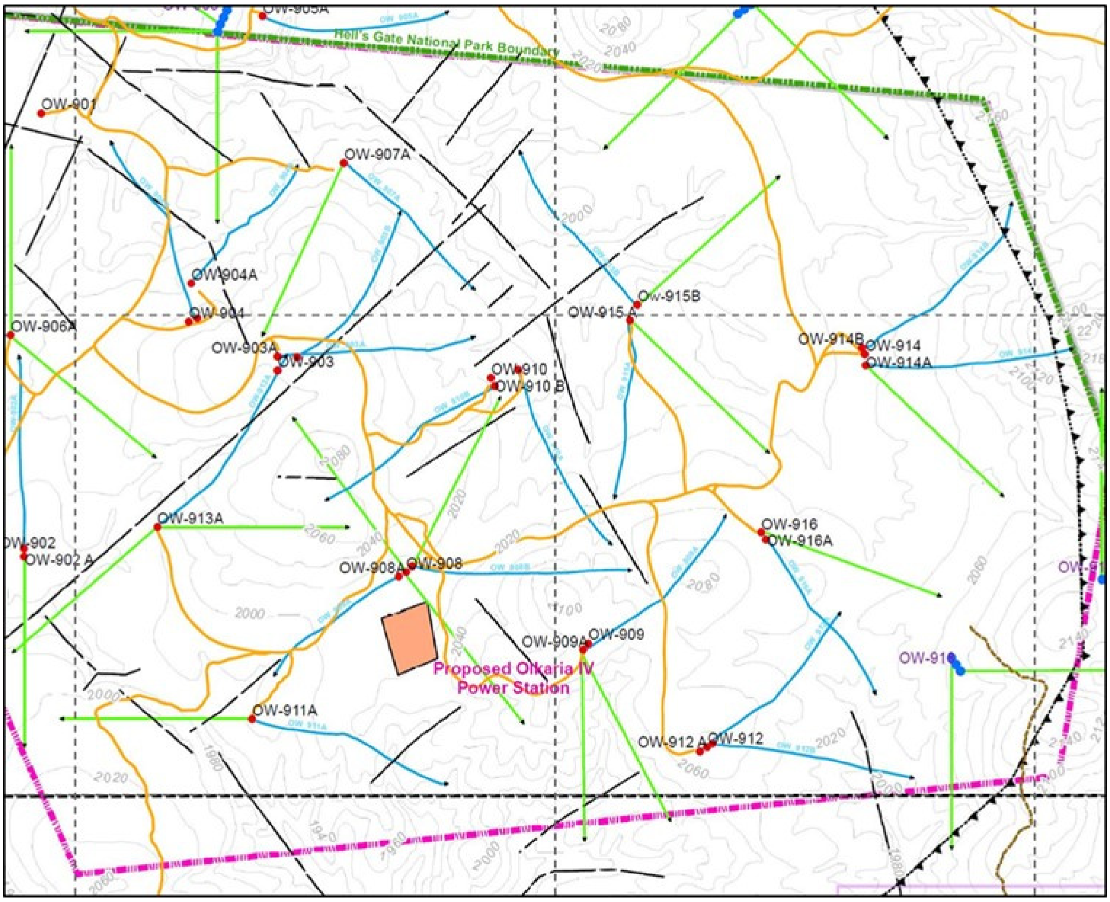

FIGURE 3: Map showing the location and well path of OW-911A in the Domes area; blue lines indicate the direction of the drilled wells; green lines indicate the proposed direction of drilling; the pink line demarcates the boundary of Olkaria Domes field; black lines indicate faults (KenGen, unpublished data)

(Figure 3). Subsurface faults have been encountered in most Olkaria wells as reported in geological well reports (e.g. Ryder, 1986; Mungania, 1992; Lagat, 1998). Figure 4 shows the actual drilling progress as compared to the planned trajectory.

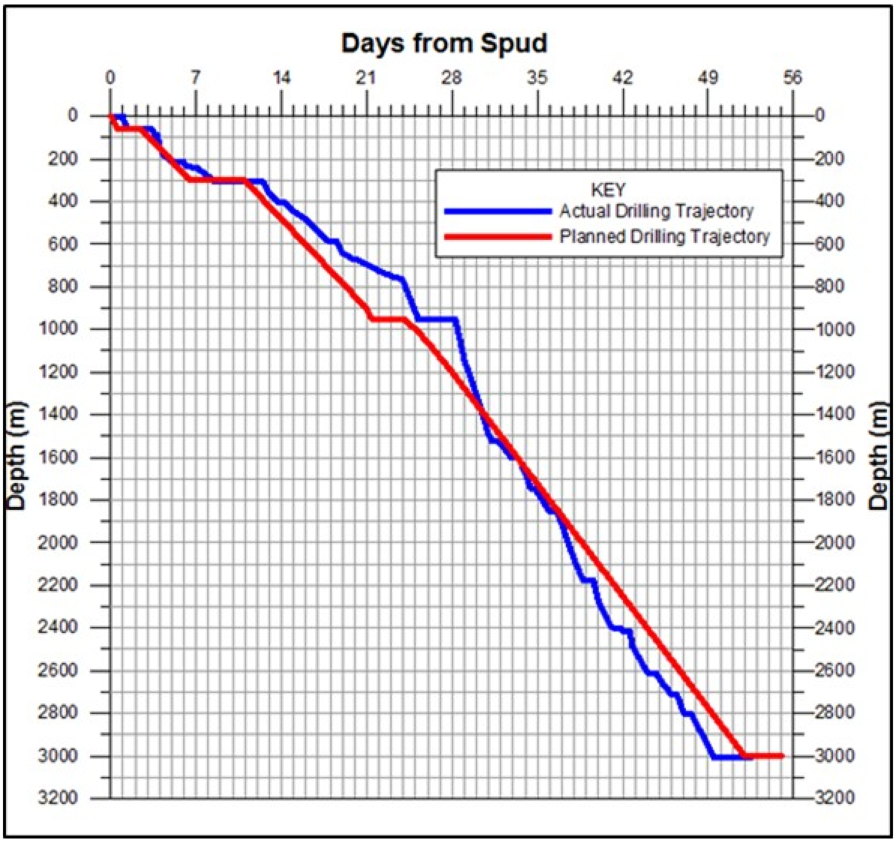

FIGURE 4: Drilling progress of well OW-911A (KenGen data, unpublished)

Spudding and drilling of the well commenced on the 4th of April 2009 and the well was completed on 26th May 2009. The injectivity test conducted at the completion of drilling measured 86.95 lpm/bar (Mwarania, 2010). Drilling was carried out in four phases:

Phase I: Drilled 26" hole from surface down to 61.1 m with mud as the drilling fluid, receiving returns to the surface. The hole was circulated to clean it, then the string was pulled out of hole (POOH). Subsequently the well was cased with 20” pipes. The hole was circulated with low viscous mud. Primary cementing was done and cement returns were received on the surface. A total of 15.02 tons of neat cement was used in the primary cementing job; then the first backfill was conducted. Cement was allowed to set for 2 days before resuming drilling.

Phase II: Drilled 17-1/2” hole in the formation from 61.1 down to 89 m with water, showing good returns. Circulation losses were encountered; at 221 m, the drill string got stuck but was freed after 8 hrs. At 237 m depth, the drilling fluid was changed to aerated water. At 305 m depth, POOH and RIH 13-3/8" casings were carried out and then the hole was circulated. Primary cementing was done and the total amount of cement used was 34.2 tons. Three backfills were done and cement was allowed to set. Drilling resumed on 16th April 09.

Phase III: Drilling resumed with aerated water and foam; the returns showed only minor circulation losses. The 1st deviation survey was conducted at a measured depth of 397 m (Angle; 3.110°, Azimuth; 224°). Then drilling of the 12-1/4" deviated hole continued from 413.1 down to 951 m without any notable loss of circulation. The hole was circulated and then POOH the drill string and the RIH 9-5/8" casings were successfully carried out without any obstruction. Primary cementing was carried out using 38.38 tons. After the 3rd backfill, drilling resumed on 1st May 2009 with aerated water and foam.

Phase IV: The drilling of the production phase kicked off with drilling an 8½" sized hole from 951 m to 3006.3 m using aerated water and foam. Deviation surveys were executed regularly so as to control the direction of drilling. Drilling continued smoothly with good returns and minor circulation losses. The total drilled depth was reached at 3006.26 m on 24th May 2009. It took three days to: POOH, run in the slotted liners, trip and prepare to log the well, perform well logging, quench to prepare for capping the well, remove the BOP and finally to install the master valve.

Temperature and pressure well logging was carried out and after 36 days, the reservoir data showed that well OW-911A was hot, with low permeability near the bottom. This was an observation based on the location of the pivot point at around 1100-1200 m depth, which indicates the location of the main aquifer (Figure 5) where pressure build-up was observed. The well's injectivity index was very low (86.95 lpm/bar), further indicating low permeability. This is the lowest injectivity value measured in the Domes field. Its transmissivity and storativity values are lower than that of the surrounding wells: OW-909, OW-908A, OW-910A and OW-912A (Mwarania, 2010).

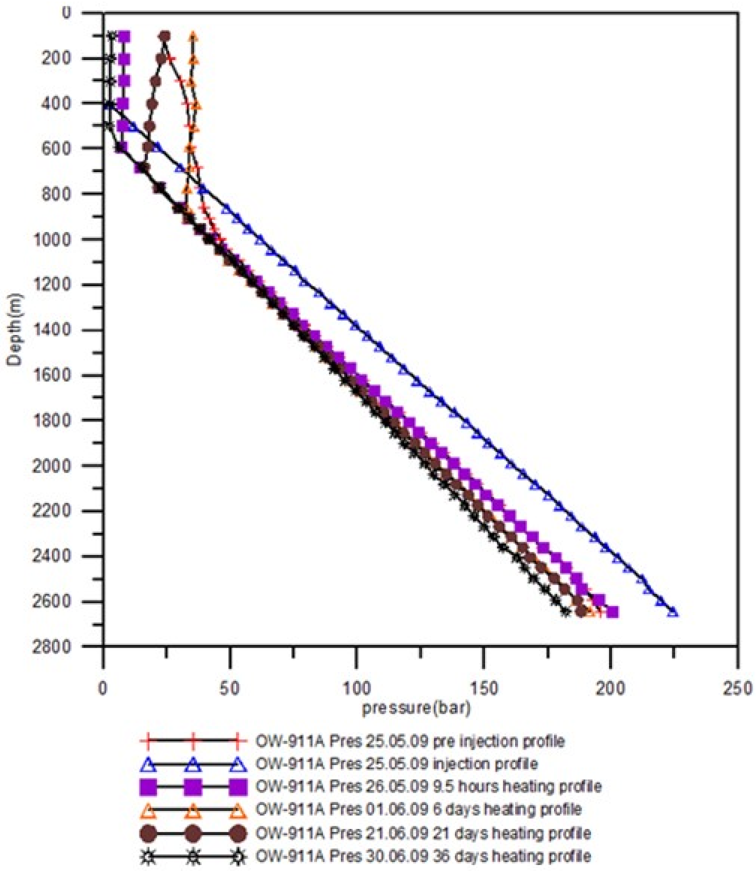

FIGURE 5: Pressure profiles for OW-911A. The pivot point in the well is probably at around 1200 m depth

4.2 Stratigraphy of OW-911A

From the binocular and petrographic analyses a lithostratigraphic succession of well OW-911A was constructed down to a depth of 3000 m, as summarised in Figure 6. LogPlot from Rockware (2007) is used for presentation of the data. The rock types encountered were pyroclastics, trachytes, tuffs, rhyolites, basalts and, to a lesser extent, syenites as dykes. Tuffs and pyroclasts are usually very porous rocks compared to basalts, trachytes and rhyolites. Permeability is mainly due to fractures. Appendix I shows a more detailed description of the stratigraphy of this well. A brief description of each rock type is outlined below.

Unconsolidated *pyroclastics* make up the top 78 m of the well. These are made up of pumice lapilli particles, obsidian, glass and lithics of probable rhyolitic composition. The bulk of the pyroclastics is poorly sorted and unconsolidated. The alteration minerals observed are chalcedony, opaques (oxides and pyrite) and clays.

Rhyolite first occurs from 282-308 m, and occurs sporadically down to 2626 m. It is pale grey to light grey in colour and occurs as fine-grained porphyritic rock. It has quartz both as a primary mineral as well as an alteration mineral appearing at about 400 m (Figure 6). Pyrite is abundant in the rocks and is found disseminated in the groundmass and also in veins. At different depths in the well, the rock shows varying alteration intensity.

According to Lagat (2004), in the Olkaria geothermal field, there are two types of rhyolites: the comenditic rhyolites which are granular non-porphyritic with abundant riebeckite and occasional hornblende. The rock is glassy and approaches obsidian in appearance; the pantelleritic rhyolites are mainly spherulitic and consist of sanidine and quartz phenocrysts, with microphenocrysts of pyroxene,

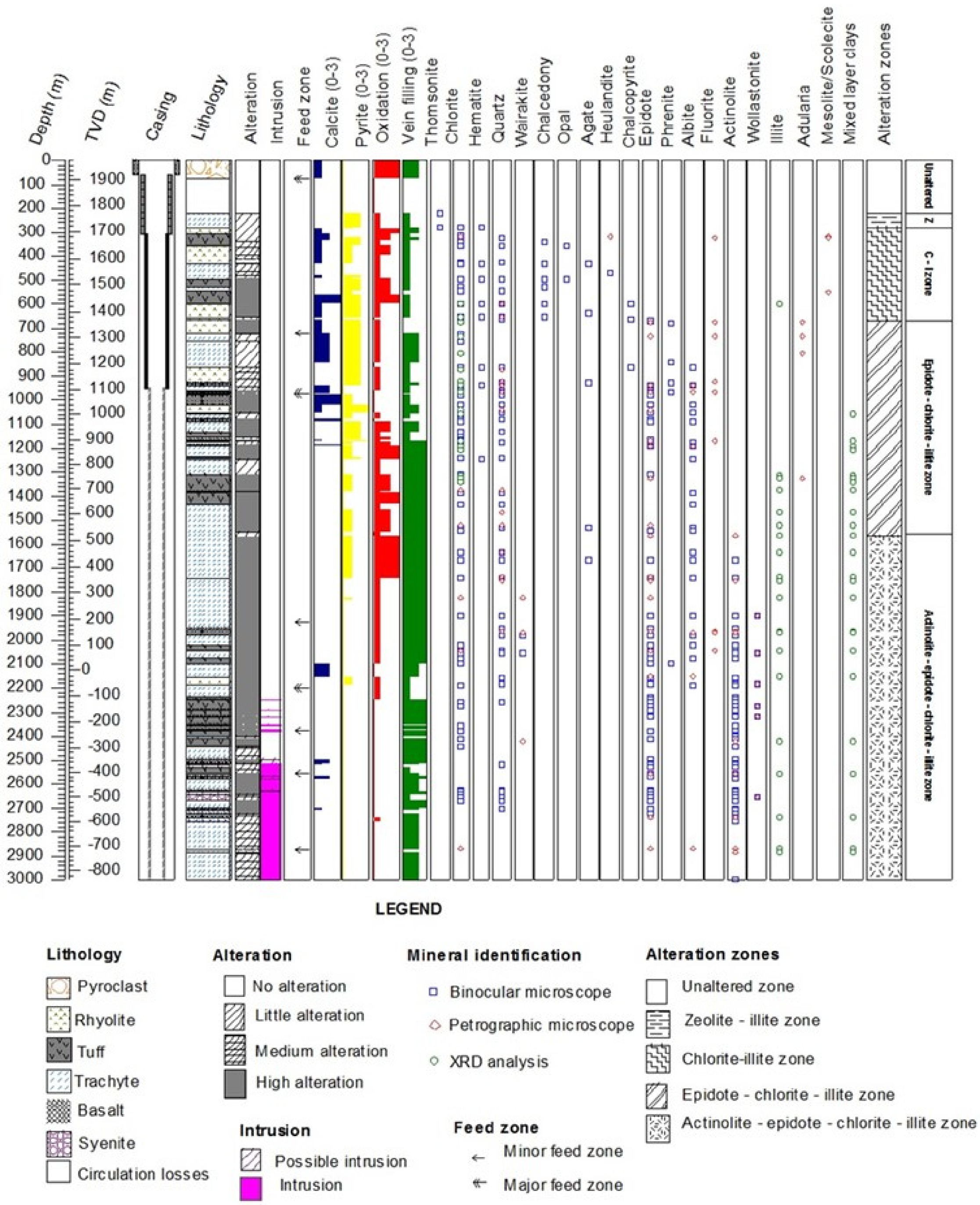

FIGURE 6: A lithostratigraphic section of well OW-911A and distribution of hydrothermal alteration

K-feldspar laths, riebeckite and magnetite. Their groundmass appears dotted with dark minerals. Both types of rhyolite were observed in well OW-911A.

Basalt first appears at 928-940 m, and keeps alternating with other rock types with depth. The rock is dark grey to greenish grey in colour, fine grained, glassy and is feldspar porphyritic. The rock generally has abundant calcite infilling veins and vesicles, but it was noted that not all the basalts had calcite since it disappeared after 1800 m. The Fe-Ti minerals in most cases show oxidation to a reddish brown colour. Alteration minerals are usually epidote with its first appearance at 670 m, chlorite and sometimes actinolite. Fresh unaltered basaltic dykes were observed at 2246-2248, 2292-2294, 2316-2318, 2352-2356 and 2370-2376 m. Highly altered basalt intrusions were observed at 2496-2512, 2564-2576, 2626-2630 and at 2700-2704 m.

Tuffs occur in thin intercalations, with the top unit at 308-356 m depth, and appear regularly down to 1450 m depth and then again at 2252-2550 m. The tuff is brown, brownish grey, grey to white in colour and occurs as two types: vitric and lithic tuff. The glassy (vitric) tuff is wholly glassy whereas the fragmental (lithic) tuff is made up of lithics of lava fragments as well as subhedral to anhedral crystal lithics of primary quartz and feldspars. The tuff occurring at depth is highly altered.

Trachyte is first seen at 222-228 m, but it dominates the lower part of the well from a depth of 1436 m to the bottom, alternating with tuff and occasional basalt. The rock ranges from grey to brownish grey in colour, fine grained and feldspar porphyritic. The rock has large sanidine phenocrysts surrounded by tiny feldspar laths exhibiting trachytic texture (flow banding). Pyroxenes and amphiboles are some of the mafics present in the rock unit.

Syenite is the plutonic equivalent of trachyte. The rock is light grey to white in colour with sanidine showing the trachytic texture. It is coarse grained, and appears sometimes fresh and sometimes altered. Syenite occurs as dyke intrusions in well OW-911A at 2512-2518, 2640-2670 and 2754-2756 m, but evidence of their strikes, dips or shapes is uncertain.

4.2.1 Lithostratigraphic comparison of wells OW-911A, OW-914A, OW-916 and OW-912B

In wells OW-911A, OW-914A, OW-916 and OW-912B below the pyroclasts above 300 m, there is a large fresh aquifer which could be due to porosity of the rocks as well as numerous fractures (Figure 7). However, this aquifer was cased off so as to avoid cooling of the well and contamination from the fresh groundwater.

Large tuff sequences at the top part of the wells were observed and seem to be the same lava flow.

An important basalt lava sequence is used as a marker horizon in the Olkaria Domes field. Figure 7 shows the lithological comparison of well OW-911A with wells OW-914A, OW-916 and OW-912B. The basalt was observed at around 500 m depth in wells OW-914A and OW-916, at 842 m in well OW-912B and 928 m in well OW-911A. This indicates that wells OW-941A and OW-916 are found at a higher elevation than wells OW-912B and OW-911A. However, it does not indicate faulting because the wells are far away from each other.

At the bottom of each well, trachyte dominates and is found to intercalate with tuff and sometimes basalt and rhyolite. This is a typical stratigraphy for wells in the Olkaria Domes.

4.3 Intrusions in well OW-911A

An intrusion is an igneous rock that is emplaced below the earth´s surface when the magma pressure breaks through the country rock. In well OW-911A, numerous intrusions are found from a depth of 2246 m (Figure 6). Most are massive and possibly dykes, made up of fresh, unaltered rocks compared to the highly altered country rock (host rock). However, at 2496-2512, 2564-2576, 2626-2630 m and at 2700-2704 m, the basaltic intrusions are highly altered. The crystallinity showed the basaltic intrusions as fine grained while the syenitic intrusions are coarse grained. The syenitic ones have trachytic texture, where the phenocrysts of sanidine occur as flow bands. Basaltic dykes are usually massive with pyroxene in the groundmass. Intrusions play an important part in a geothermal system, where they are part of the heat source; they may provide permeability along their fractured margins and they may also form a barrier for flow, perpendicular to their boundaries.

Syenitic intrusions were only observed in wells OW-911A and OW-916 below 2500 m depth. Basalt intrusions were, however, observed in wells OW-911A, OW-914A, OW-916 and OW-912B.

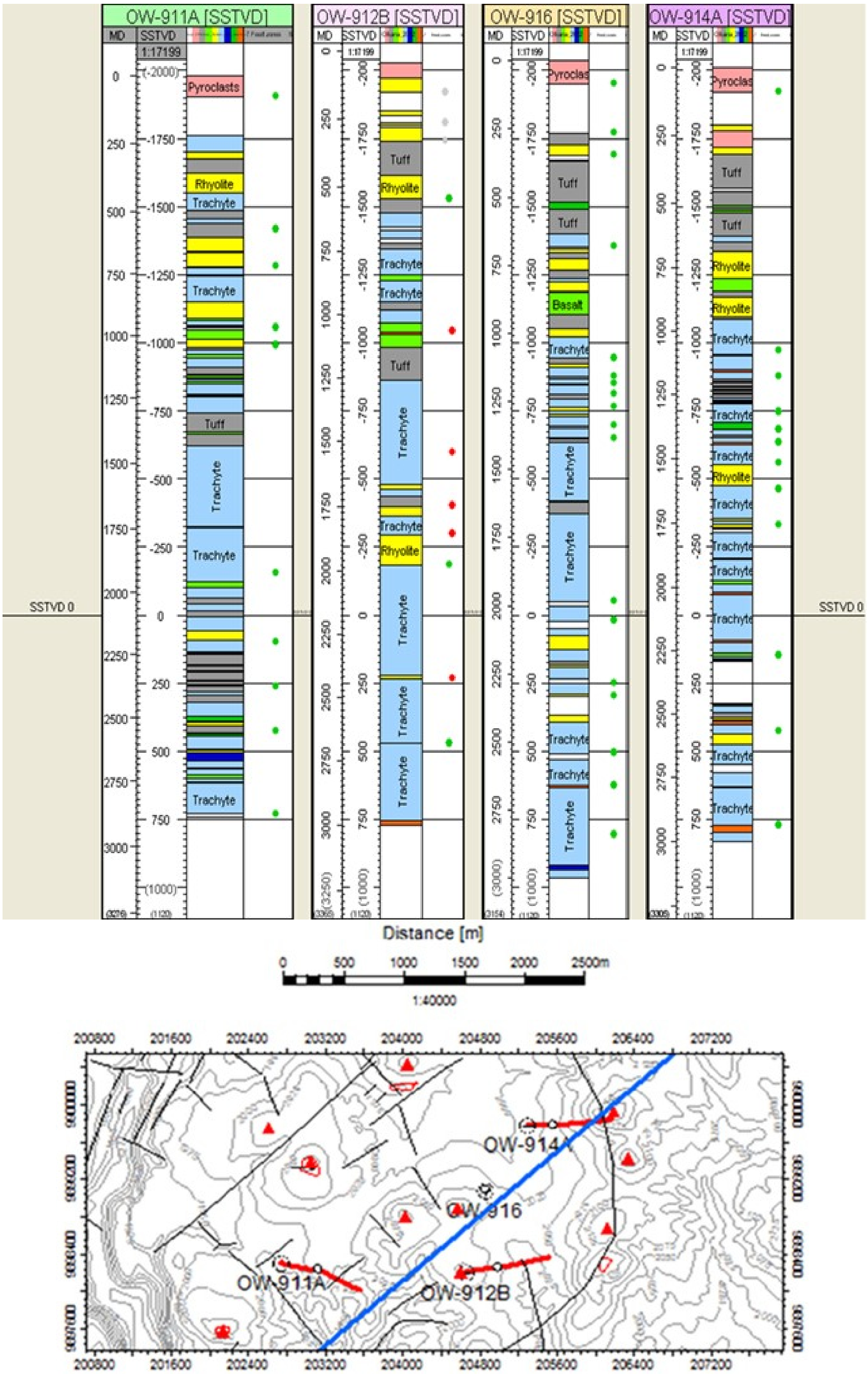

FIGURE 7: Comparison of the lithology between wells OW-911A, OW-914A, OW-912B and OW-916. The red dotted line connects a basaltic marker horizon, seen in all the wells. The lower figure shows the location of the cross-section; the red lines indicate the drilled direction of wells OW-911A, OW-912B and OW-914A. The blue line is a cross-section between these wells; the red triangles indicate volcanic centres

4.4 Aquifers in OW 911A

An aquifer is an underground water-bearing geological formation which is permeable and porous. Fresh groundwater aquifers are cased off during drilling to avoid cooling of the well and contamination from the fresh groundwater. In volcanic systems, like in Olkaria, one expects the permeability to be fracture-dominated, and those fractures are target areas when drilling production and re-injection wells. One may, in the future, look more closely at the proposed faults which appear to be present between the wells in the Domes as possible geothermal structures.

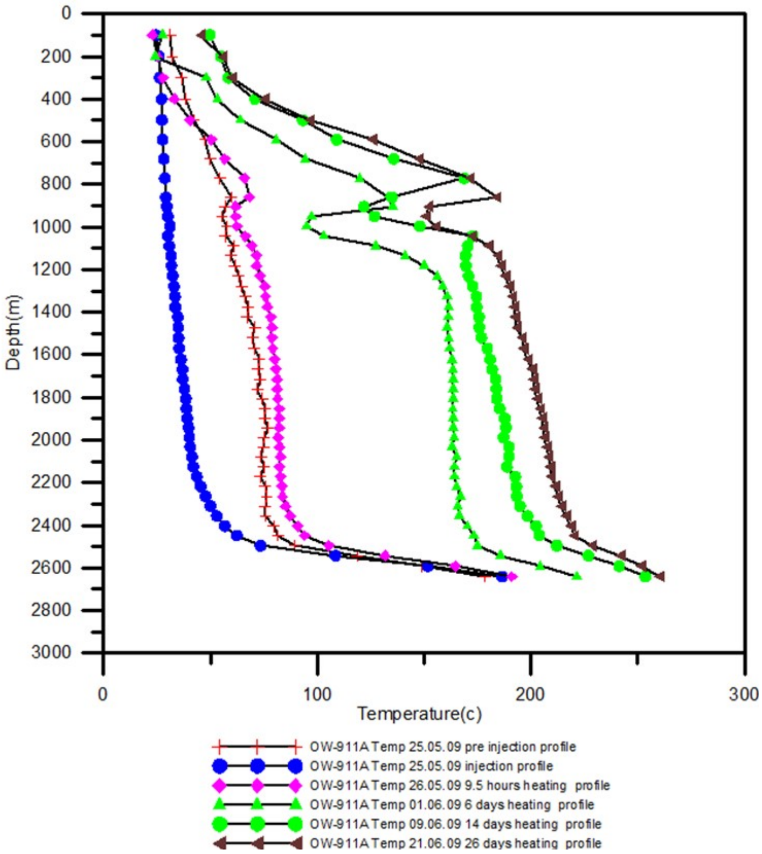

FIGURE 8: Temperature logs showing location of aquifers/feed zones

The methods used to identify aquifers and feed zones include temperature logs, circ-ulation losses, alter-ation mineral intensity and penetration rates. However, caution must be taken regarding circulation losses when drilling is executed with aerated water.

The identification of aquifers in this well was nearly exclusively from temperature log data, shown in Figure 8. The main aquifers were located based on cooling points or consistent temperature deflections between individual logs. On these grounds, a temp-erature drag at 970 m and a rapid increase in temperature at 2200 m were found, while minor feed zones were found at 1924, 2070, 2378 m and 2554 m.

The well remained relatively tight during drilling and most of the apparent circulation losses only occurred over short periods of 2-4 m depth intervals and may have been caused by air pockets in the well during drilling. However major losses took place at 78-222 m and 2876-2886 m, although the former depth had to be cased off due to a fresh groundwater aquifer.

Areas with abundant actinolite and epidote as vein fillings may possibly indicate feed zones, but will have to be looked at more closely later. Most of the feed zones, with the exception of the one near 1100 m, were found at varying depths between1900 m down to 2876 m, as can be seen in Figure 6.

A total of 8 feed points were observed. As these are mostly determined on the grounds of temperature logs that are point measurements at 50 m interval, some margin of error must be accounted for in precise locations; this, in turn, makes a comparison with the geological context in the well more difficult.

In Figure 9, the feed zones of wells OW-911A, OW-914A, OW-912B and OW-916 are shown. Well OW-914A cuts through a high permeability zone at about 2290 m depth, accompanied by an increase in alteration intensity. It has been proposed that this may be the dome ring structure at a depth of 2290 m; at this depth circulation losses occurred, but slightly, before the intensity of alteration minerals increased significantly. Wells OW-912B and OW-911A are drilled directionally to the southeast to target the NE-SW and Domes ring structure, but they do not cut any major faults.

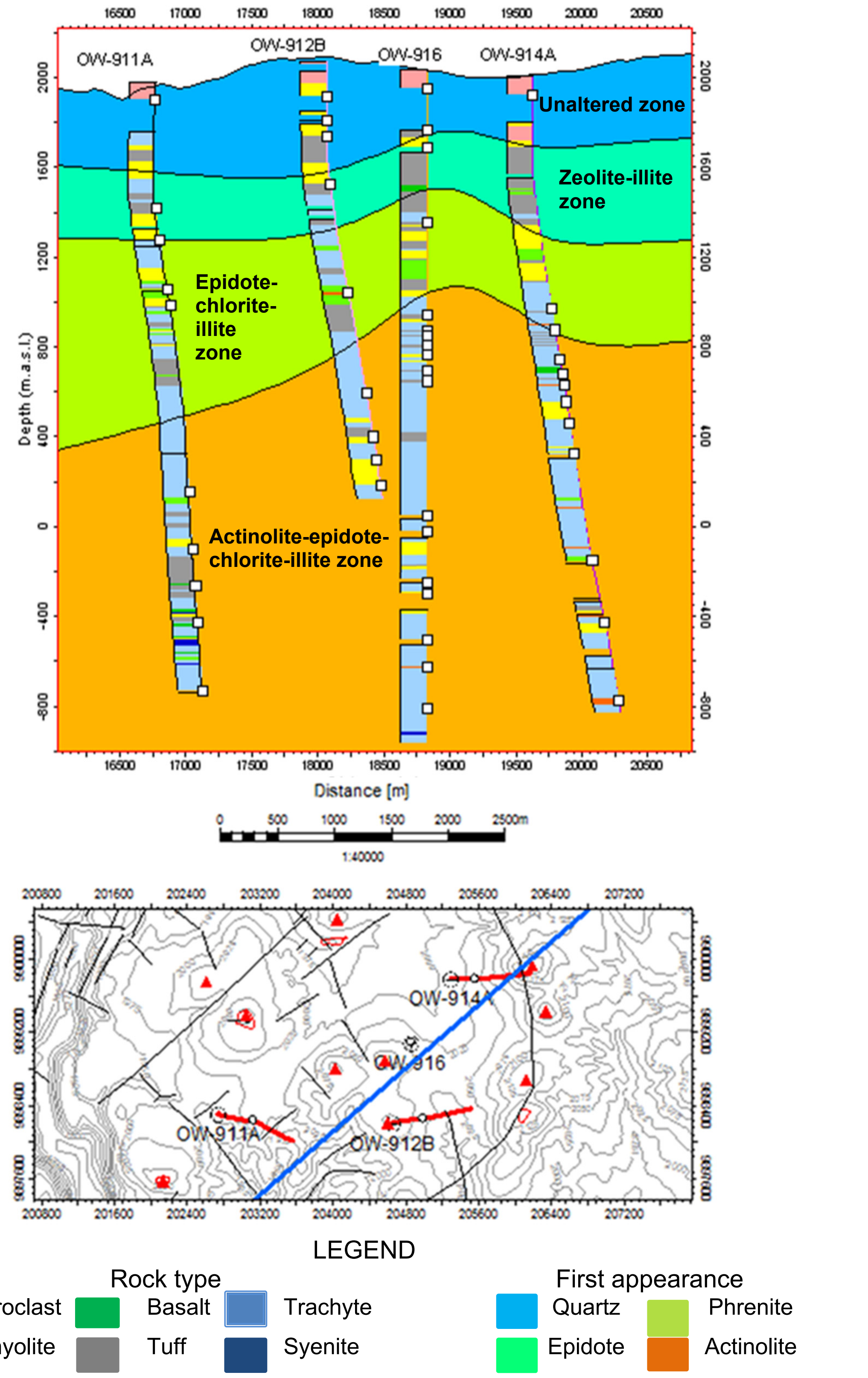

FIGURE 9: Comparison of hydrothermal mineral alteration between wells OW-911A, OW-914A, OW-912B and OW-916; aquifers are indicated by white rectangles. The lower figure shows the location of the cross-section; the red lines indicate the drilled direction of wells OW-911A, OW-912B and OW-914A; the blue line is a cross-section between these wells; red triangles indicate volcanic extrusive centres

5. HYDROTHERMAL ALTERATION

5.1 Alteration of primary minerals in OW-911A

In Olkaria, the major rock types are trachyte, rhyolite, tuff and basalt. Trachytes usually consist mainly of feldspars, pyroxenes and opaques. Rhyolite is composed mainly of quartz and feldspar minerals, and there are only traces of amphiboles and pyroxenes. The groundmass of basalt generally consists of pyroxene, plagioclase and minor olivine (Omenda, 1998). Tuff is predominantly of glassy material.

The order of alteration depends on the Bowens reaction series so that the first mineral to be formed is also the first to be altered (Figure 10). Volcanic glass cannot be classified as a mineral but is relevant in this discussion as its replacement products are quite relevant as hydrothermal minerals (Njue, 2010).

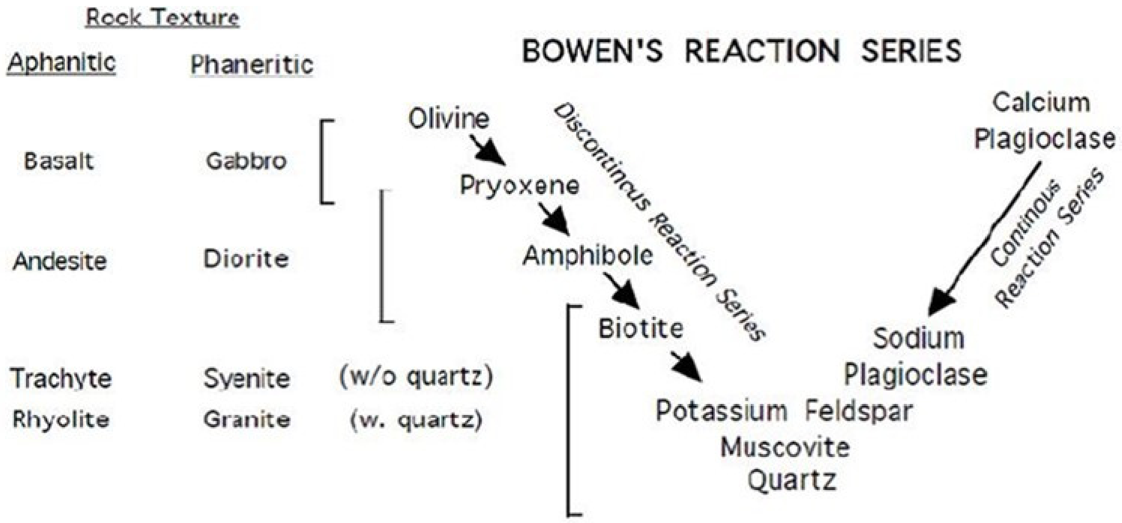

FIGURE 10: Bowen's reaction series (Thomas, 2010)

Volcanic glass: Obsidian volcanic glass, as well as vitric tuff, comprises common volcanic rocks in Olkaria. Volcanic glass has concoidal fractures and the perlitic texture can be seen as a relic even when the rock is altered. Glass alters to zeolites, opal, agate, chalcedony, clays and may even be replaced by calcite. Thomsonite can be seen at 222 m, while agate and chalcedony occur from 222 m down to 634 m. These low temperature minerals are commonly found at shallow depths but disappear downwards due to increasing temperatures in the formation. Abundant calcite may indicate permeability, especially if it is a contact zone like at 560 m. The platy calcite found at 668 and 750 m indicates boiling, which could fit with the temperature curve in Figure 11.

Olivine: Is a primary mineral in basalt and is highly susceptible to alteration (Table 1). This is because it is usually the first mineral to crystallise during formation of the rock, according to the Bowen's reaction series. However, more evolved basalts are olivine-free. In Olkaria, all the olivine in the rocks has been altered. It alters to chlorite, actinolite, hematite and clay minerals.

Feldspar: Is commonly found as a major groundmass component as well as phenocrysts in trachytes and basalt. It appears as a milky white to transparent mineral. The feldspars are of two types, either Ca-Na plagioclases or K-Na alkali feldspars. Feldspars may also alter to calcite, epidote and occasionally to warakite and chlorite. Plagioclase feldspar alters to albite and may also alter to adularia, especially at zones of high permeability (Browne, 1984a; 1984b). Replacement to actinolite is observed at 1556 m. The intensity of alteration is relatively high and can be seen at different depth intervals throughout the well. Abundant calcite and epidote as vein fillings may indicate permeability, as indicated at 2430 m.

Pyroxene: Is very common in basalt and occurs both as a groundmass and as phenocrysts. It appears in binocular analysis as a black mineral with a metallic lustre. It alters to clays and actinolite.

Opaques: They occur as dark minerals in the rocks. FeTi-oxide is the most common in basalt and trachytes and is quite resistant to alteration. It alters to sphene and hematite and is replaced by pyrite. Abundant pyrite may indicate a permeable zone, e.g. at 2200 m.

TABLE 1: Primary minerals and their alteration minerals in well OW-911A

Susceptibility	Primary rock minerals	Alteration minerals
Decreasing ↓	Volcanic glass	Zeolites, chlorite, opal, agate, chalcedony, clays
	Olivine	Chlorite, actinolite, hematite, clays
	Feldspar	Adularia, calcite, warakite, chlorite, epidote
	Pyroxene	Actinolite, clays
	Opaque (magnetite)	Sphene, hematite, pyrite

5.2 Hydrothermal alteration minerals in well OW-911A

In the Olkaria geothermal system, glass and olivine are usually the first phases to be altered at low temperatures from about 50°C. Calcite, clays and pyrite are the most common alteration minerals in well OW-911A, followed by thomsonite, a zeolite, at 222 m, quartz at 400 m, epidote at 670 m, and actinolite and wollastonite at 1556 m, as summarised in Figure 6. Characteristic features of the main alteration minerals found in the well are described below, with some general descriptive points by Saemundsson and Gunnlaugsson (2002).

Opal is a silica mineral that is almost amorphous. It is softer and less dense than other silica minerals and forms at temperatures less than 100°C. It was noted at 326 m using binocular analysis. It is common at shallow depths and disappears completely after 526 m. It is common in the tuffs and rhyolites.

Chalcedony is also a silica mineral which is translucent with a slightly vitreous lustre. It is commonly whitish or greyish in colour. The most abundant type in well OW-911A is botryoidal chalcedony. It is a low-temperature alteration mineral and forms at temperatures ranging from 70 to 180°C. It was noted at 342 m using binocular analysis. It is common at shallow depths and disappears completely after 660 m. It is common in the tuffs and rhyolites.

Agate is a variant of chalcedony with bands of different colours, occurring as an amygdule, generally following the contours of the vesicle, forming a concentric pattern. It was found at 432 m using binocular analysis. It is common at shallow depths and disappears completely after 660 m. It is common in the tuffs, basalts and rhyolites.

Zeolites are a category of hydrous secondary minerals composed of Na, K and/or Ca-Al silicates. They are often classified by their shape into three main categories: fibrous, tabular/prismatic and granular. They are formed during alteration and precipitation in vugs and vesicles as hydrothermal fluids dissolve various substances from the rock. On cooling, the minerals precipitate to form amygdules and vein fillings. They are low temperature minerals except for wairakite, forming at less than 180°C (Saemundsson and Gunnlaugsson, 2002).

Thomsonite is a typical radial zeolite. It radiates in clusters from a single point. It is usually milky white, and the variant has thinner fibres. It indicates low temperatures of about 60-120°C. It occurs at 222 m depth in the binocular microscope. They are only found at shallow depths and occur in all rock types.

Heulandite forms tabular crystals. It is translucent or transparent in newly opened cavities. Generally, it forms relatively thick trapezoid aggregates or clusters with truncated points. The crystal form is sometimes referred to as coffin-shaped. It cleaves easily with a strong pearly lustre on cleavage surfaces. It indicates an alteration temperature of about 60-120°C. Heulandite was found in a trachyte at 468 m using the binocular microscope.

Wairakite is a granular zeolite which forms colourless or white trapezohedral crystals with a vitreous lustre. It occurs either as individual crystals or as clusters which glitter as seen in binocular microscope. It is stable at a temperature range of 200-300°C. It was found at five locations below 1820 m using both the binocular and petrographic microscopes.

Quartz is colourless and transparent, forming prisms with a regular hexagonal pyramid shape when it is a secondary mineral. The prism is generally whitish or greyish while the point is transparent. It forms at temperatures of more than 180°C. It is difficult to differentiate it from primary quartz, but the hexagonal shape is the best way to differentiate between the two especially, in the binocular microscope. It was observed both in petrographic and binocular analysis starting at 340 m and is present down to the bottom of the well. It is most commonly observed in rhyolites, basalts and tuffs.

Adularia, as seen in the petrographic analysis, occurs as a replacement of sanidine and is occasionally deposited in veins. It was found at four locations, mainly though between 680-800 m and then at around 1400 m. Adularia has often been associated with high permeability (Browne, 1984b). The feed zone at about 700 m may attest to that.

Albite is seen to form deeper than adularia at a depth of 940 m using a petrographic microscope. Albitization refers to the replacement of primary plagioclase. Albitised plagioclase has a low refractive index and shows no zoning but a typical chessboard-like twinning (MacKenzie and Guilford, 1980). It is found at varying depth intervals down the well. It is mostly found in the interval from about 900 m down to 2200 m depth, with only one occurrence below that.

Calcite is generally white but may be coloured by impurities. It normally has a vitreous lustre and has good cleavage. The easiest way to identify it in binocular analysis is to douse the sample with a diluted HCl solution; calcite will effervesce if present. Calcite appears to be most dominant between 300 and 1200 m in the well; this appears to be the typical distribution among the other three Domes wells. It is found sporadically below 2200 m depth and may associate, possibly in two instances, with aquifers there. Platy calcite was observed at 668 and 750 m by binocular analysis. This may be an indication of boiling in the system.

Fluorite is an isotropic mineral (Kerr, 1977) and is seen to be transparent with good cleavage when viewed with plane polarised light. It first occurs at 324 m and can be seen at various depths.

Hematite is an anhydrous iron oxide. It occurs in various forms. When coarsely crystalline, it is steel grey or blackish, sometimes with a bluish or multi-coloured sheen with a metallic lustre. Using binocular microscope, hematite was observed sporadically in cuttings from a depth of 282 down to 1246 m. The knobby variant was observed at 940 m. It is formed from the oxidation of magnetite. It occurs in trachytes, tuff and basalt.

Pyrite is a brassy yellow, cubic, commonly euhedral mineral, readily identified by its colour and shape and occurs below about 222 m and is common down to about 1200 m, below which its abundance decreases gradually down to about 1700 m. Below that depth it is only found at two locations, the latter coinciding with or being near to a feed zone at 2150 m. It was associated with calcite down to a depth of 1192 m. Its presence in abundance commonly indicates permeability, which may comply in this well as permeability is low in the lower part of the well. It occurs in all rock types.

Epidote is generally microcrystalline with a yellowish-green colour in cuttings. It forms at temperatures of about 240°C and above. It displays strong pleochroic green colours in thin sections. It precipitates as fillings in vesicles in the upper part of the well, and as vein fillings near the bottom of the well; this indicates possible feed zones. It is sporadic from 670 down to about 900 m where it becomes more abundant all the way to about 2750 m where it mostly disappears. The first occurrence of crystalline epidote in Olkaria is used as an indicator that a well has reached the production zone.

Prehnite forms crystals with vitreous lustre. It is often colourless and transparent. It occurs with epidote and forms at ~240°C and higher temperatures. It was only found at three locations between 680 and about 1000 m and in one location at 2100 m depth.

Actinolite belongs to the amphibole group. It is an alteration mineral of pyroxene and is also found as a vug mineral. Crystals are generally very slender fibres, often radiating with vitreous lustre. It is greenish, blue or grey in binocular analysis. It forms at a temperature above 280°C and was first encountered at 1562 m depth in thin section and sporadically down to 1950 m, below which it becomes more common down to 2800 m; below that it was only seen at one location.

Wollastonite is fibrous and white and occurs with actinolite at depth. The major structural difference when compared with actinolite is that the thin fibres of wollastonite radiate in many different directions while the actinolite fibres show a more parallel arrangement. It was found at four locations from 1900 m down to about 2300 m, but only at one location below that.

Clays are mainly formed by hydrothermal alteration of the country rock. They are used as temperature indicators in geothermal systems. They are identifiable using binocular, petrographic and XRD analyses. XRD analysis is usually the best and most consistent method used to identify clays. The most common clays in well OW-911A were chlorite, mixed-layer clay and illite. Appendix II shows characteristic peaks of XRD analyses for these clays.

> *Chlorite* is pale green in colour and has a fibrous clay structure when viewed under plane polarised light in a petrographic microscope. It forms above 190°C (Saemundsson and Gunnlaugsson, 2002). It is formed by the alteration of rock-forming minerals, as amygdules and on fissure surfaces. XRD analyses of chlorite show conspicuous peaks at 7.0-7.2 and 14.0-14.5 Å in the untreated, glycolated and oven heated samples. It was first observed at 598 m in XRD, but from 282 m in binocular and petrographical microscope.
>
> *Mixed-layer clay* for chlorite /illite was observed using XRD analysis, and the peaks were between 12.0 and 12.5 Å in the untreated, glycolated and oven heated samples. The first appearance was at 1318 m down to 2900 m, indicating temperatures of up to 200°C.
>
> *Illite* is light green to white in colour, replaces glass and feldspar and also occurs as a vein- and vesicle-filling mineral. XRD analyses of illite show a peak at the 10 Å in the untreated, glycolated and oven heated runs. Illite is stable at temperatures higher than 200°C. It was first observed at one depth at 600 m but then not again until at 1300 m. There it is common down to about 1800 m, below which it becomes more sporadic.

5.3 Veins and vesicle fillings

Vesicles are pores formed in the rock during an eruption as gas exsolves from magma, while veins are micro fractures in the rock and can occur due to primary jointing in the rock or later tectonic fractures. They imply porosity and permeability in the rock. When the hydrothermal fluid passes through the veins and vesicles, it alters the rock and precipitates hydrothermal minerals. During the binocular and petrographic analysis, the alteration minerals found within the vesicles help to decipher the formation temperature. Veins can be detected using binocular analysis when the alteration minerals cover the side of a rock fragment, when they are found as a whole mineral fragment in the cuttings, and when the veins in the rock cuttings are filled with an alteration mineral. Veins indicate feed zones.

Vesicles are mainly found in tuffs, rhyolites and trachytes. At 222 m, thomsonite was seen as an amygdule. Vesicle fillings are common at shallow depths, predominantly with zeolites and clays. An abundance of vein fillings were observed with depth, as shown in Figure 6. These veins are most abundant between about 1200 down to 2100 m but seem to diminish below that.

5.4 Alteration mineral zones of well OW-911A

From the binocular, petrographic and XRD analysis results, four mineral alteration zones were identified. The boundary between one zone and another is defined by the first appearance of a thermally dependent mineral. XRD results are shown in Appendix II.

Unaltered zone (0-78 m): The rocks in this zone are relatively unaltered, but highly oxidised. Alteration that could be related to hydrothermal activity was not observed in this zone.

Zeolite – illite zone (222-282 m): Zeolites are low-temperature minerals. Thomsonite was first observed at 222 m. This zone indicates alteration temperatures between 50-200˚C.

Chlorite – illite zone (282-670 m): This zone is marked by the first appearance of chlorite (using binocular analysis) at 282 m. In XRD analysis, it was observed at 598 m. Chlorite and illite clays indicate alteration temperatures of about 200°C.

Epidote – chlorite – illite zone (670-1562 m): The appearance of crystalline epidote marks the upper boundary of this zone. The first occurrence was found in cuttings with binocular analysis at 670 m depth. It indicates an alteration temperature of more than 240˚C.

Actinolite -epidote – chlorite – illite zone (1562-3000 m): The first appearance of actinolite was used to mark the upper boundary of this zone. It was first observed at 1562 m in thin section. It indicates an alteration temperature of 270˚C and more.

A cross-section was done in order to compare the alteration zones of neighbouring wells OW-911A, OW-912B, OW-916 and OW-914A (Figure 9). It shows that wells OW-916 and OW-914A are located closer to a heat source, or up-flow zones in this area of the Domes, while well OW-911A is located farther away from the heat source. For example, Figure 9 shows clearly that actinolite occurred at a much shallower depth, i.e. 1030, 1218 and 1260 m, in wells OW-916, OW-914A and OW-912B, respectively, while in OW-911A it occurred first at a much deeper level at 1562 m.

5.5 Mineral deposition sequences of OW-911A

A relative time scale of mineral deposition can be deduced from veins and amygdules. The oldest minerals form at the edges of amygdules, while the youngest form in the centre. This information is useful since it tells us whether the system is cooling down, heating up or if it is at equilibrium. If the system is heating up, the mineral at the centre will be a higher temperature mineral than the one at the edge and, if the system is cooling down, the reverse will be observed. A mineral sequence can also be deduced from cross-cutting of veins; if a vein filling cross-cuts another vein or another mineral, then it is younger than the one being cross-cut.

For well OW-911A, the mineral sequence was studied petrographically. However, alteration mineral sequences were rarely observed. The ones that were seen are summarized in Table 2. The mineral deposition sequence shows e.g. that low temperature zeolites, like mesolite-scolecite, form later than chlorite, a high-temperature clay, at shallow levels of about 320 m. This depositional sequence indicates that chlorite formed at an earlier time and that, subsequently, the well at this level cooled down emplacing zeolite under lower temperature conditions. However, deeper in the well the system progressively evolves to form high temperature minerals like prehnite, epidote, wollastonite and actinolite (Table 2).

TABLE 2: Sequence of alteration mineral deposition in well OW-911A

Depth (m)	**Lithology**	**Alteration intensity**	**Alteration sequence** **Older ⟶ Younger**
320	Tuff	Low	Chlorite-mesolite/scolecite
554	Tuff	Low	Chlorite-quartz
968	Basalt	Medium	Quartz-epidote
1244	Rhyolite	Medium	Quartz-chlorite
1820	Trachyte	Medium	Chlorite-epidote-actinolite
2150	Trachyte	Medium	Prehnite-chlorite
2250	Tuff	High	Epidote-actinolite-wollastonite
2422	Trachyte	High	Actinolite-chlorite
2558	Trachyte	High	Epidote-prehnite-actinolite
2630	Rhyolite	High	Chlorite-epidote-actinolite

5.6 Fluid inclusions in well OW-911A

A fluid inclusion is a small bubble of water and/or gas and steam trapped inside a crystal structure. The fluid inclusion can be primary, which means that it formed during the crystallisation of the mineral, or it can be a secondary inclusion, which means that it was trapped in a fracture, which later healed. Fluid inclusions with vapour bubbles can be used to determine the temperature of homogenisation (T_h), which is usually close to the temperature at which the fluid was trapped. It indicates temperature of the system at that time. Fluid inclusions can be found in many types of minerals but usually they are analysed in calcite and quartz.

Fluid inclusion analysis was done in two crystals of quartz and calcite picked out from cuttings at 1050 m depth. The total number of measurements was 15 with the highest temperature at 286°C. Figure 11 shows the relationship between formation-, boiling point curve-, fluid inclusion- and alteration mineral temperatures of well OW-911A at different depths.

The alteration mineral temperature curve is slightly higher than the formation temperature by 40°C. This indicates that the well has been cooling. Below 1050 m depth, the alteration mineral temperature curve and the boiling point curve have the same temperature; this indicates that the well is in a state of equilibrium. Fluid inclusion temperatures are almost at equilibrium with the boiling point curve and the alteration mineral temperature curve. This indicates that the formation temperatures have been underestimated, but these temperatures are calculated according to the level of heating up of the well with time. If the well is not allowed to heat up sufficiently before temperature loggings are conducted, the formation temperatures will appear low. The temperature history of this well indicates that there may have been some cooling in the top part of the well but, at depths below about 500 m, the well has attained equilibrium.

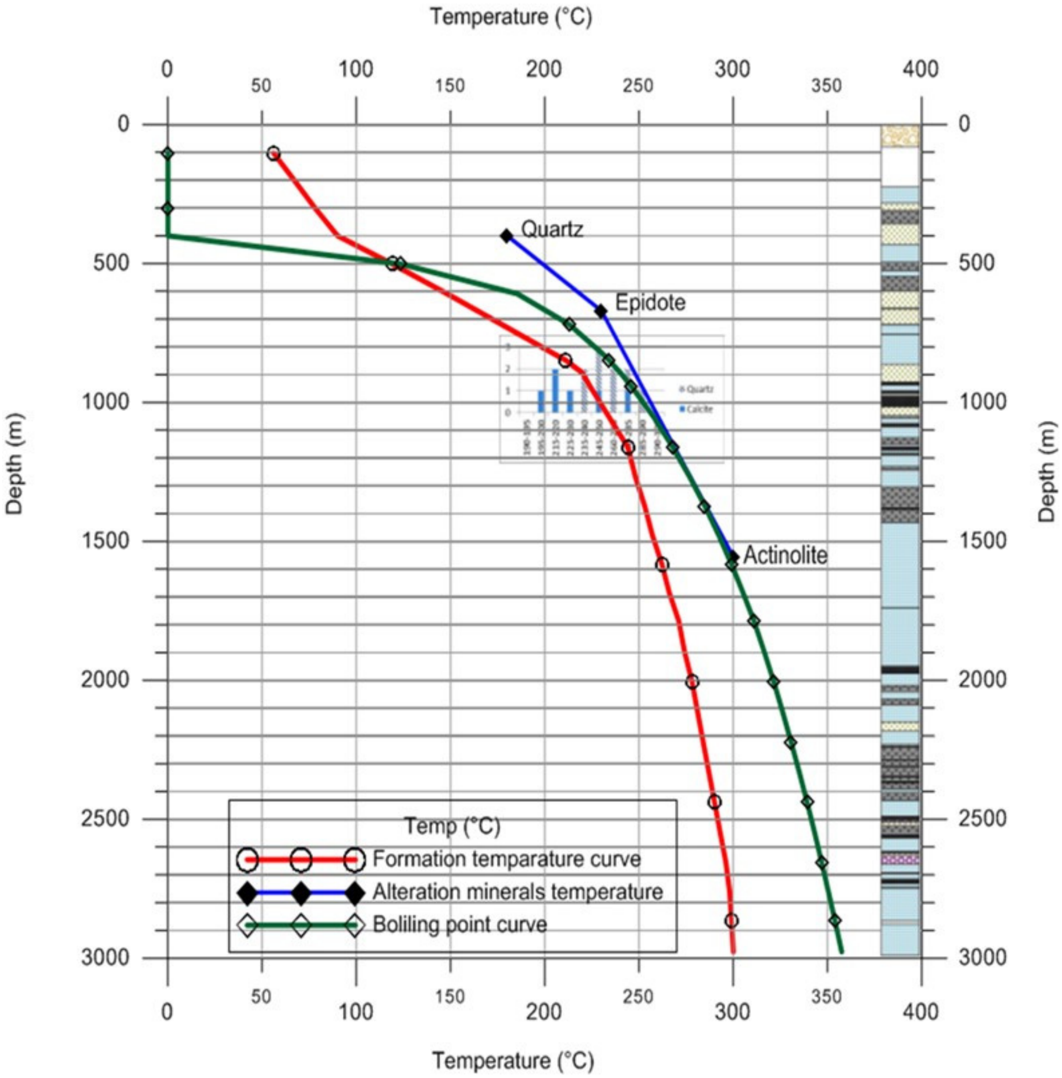

FIGURE 11: The relationship between fluid inclusion temperature, alteration mineral temperature and the boiling point curve for well OW 911-A; the formation temperature curve was calculated and as heat-up times between temperature logs were short, the curve may be inaccurate, probably showing too low temperatures; the well may not have reached equilibrium with the surrounding rock formations

6. DISCUSSION

The stratigraphy of well OW-911A shows that the top 78 m are made up of unconsolidated pyroclastics, while trachyte was found to dominate the lower part, intercalating with tuff and occasionally basalt. Trachyte, which is presumed to be the reservoir rock, dominates below 1436 m. Numerous dyke intrusions of syenite and basalt were noted at depth. Basaltic dykes could be seen at 2246-2248, 2292-2294, 2316-2318, 2352-2356, 2370-2376, 2496-2512, 2564-2576, 2626-2630 and 2700-2704 m. Syenitic dykes occur at 2512-2518, 2640-2670 and 2754-2756 m.

Four major alteration zones were observed, defined by the first appearance of a dominant temperature dependent mineral: unaltered zone between 0-78 m, zeolite – illite zone between 222 and 282 m, chlorite – illite zone between 282 and 670 m, epidote – chlorite – illite zone between 670 and 1562 m, and actinolite – epidote – chlorite – illite zone between 1562 and 3000 m.

Aquifers and feed zones were identified using temperature logs, circulation losses and the abundance of alteration minerals, in particular as vein fillings. A total of 8 feed zones were observed (Figure 6). The well did not hit the intended NW-SE striking structures seen at the surface, indicated by the fact that there were no major circulation losses and also that according to reservoir data, the well is impermeable at depth. There are abundant vein fillings at depth but there is almost no permeability below 2500 m, possibly due to the numerous intrusions which may act as barriers to permeability. The major sources of permeability in the well are mainly along fractures/faults, indicated by circulation losses at 78-222 m, temperature drag and a rapid increase in temperature in the temperature logs at about 970 m and 2200 m, respectively.

The mineral deposition sequence shows that low temperature zeolites like mesolite-scolecite form at the same shallow depths of less than 500 m as chlorite, a high-temperature clay. This depositional sequence indicates that chlorite formed at an earlier time; then the well cooled down emplacing zeolites under lower temperature conditions. However, the system is progressively evolving to form high temperature minerals like prehnite, epidote, wollastonite and actinolite at depth.

The subsurface temperature distribution was estimated from hydrothermal alteration mineralogy, fluid inclusion measurements, temperature logs from temperature recovery tests, and the pressure profile plot (Figure 5). After compiling these different data, it was concluded that the well is hot with temperatures up to 375°C, according to the boiling point curve and alteration mineralogy temperatures (Figure 11). However, the bottom of the well is impermeable. According to alteration mineral temperatures and the fluid inclusion temperatures, the temperature history of this well indicate that there has been cooling in the top part of the well, but the well has attained equilibrium at deeper levels.

Well OW-911A is located farther away from a potential heat source than wells OW-916, OW-912B and OW-914A. This was deduced from the fact that the first occurrence of high temperature alteration minerals, like actinolite and epidote, occurred at shallower depths in wells OW-916, OW-912B and OW-914A than in well OW-911A (Figure 9).

7. CONCLUSIONS

- The rocks encountered in this well include pyroclastics, rhyolites, tuffs, syenites, trachytes and basalts.

- Hydrothermal alteration mineralogy indicates temperatures of more than 250°C below 670 m, as evidenced by well crystalline epidote, and >300°C below 1562 m, as evidenced by the presence of actinolite and wollastonite.

- The major alteration zones encountered in this well are: unaltered zone between 0 and 78 m, zeolite – illite zone between 222 and 282 m, chlorite – illite zone between 282 and 670 m, epidote – chlorite – illite zone between 670 and 1562 m, and actinolite – epidote – chlorite – illite zone between 1562 and 3000 m.

- Syenites and basaltic dykes are the major intrusive rocks which characterise well OW-911A.

- Major sources of permeability in the well are mainly along fractures/faults, indicated by circulation losses at 78 m, temperature drag and a rapid increase in temperature in the temperature logs at about 970 and 2200 m, respectively.

- The well is located farther away from the potential heat source when compared to wells OW-916, OW-914A and OW-912B and has almost no permeability below 2500 m. It is possible to find permeability in the opposite direction to target the NE-SW trending faults.

ACKNOWLEDGEMENTS

I would like to thank my employer, Kenya Electricity Generating Company - KenGen, for granting me the opportunity to attend this training programme. I am thankful to Dr. Ingvar B. Fridleifsson, the Director, and Mr. Lúdvík S. Georgsson, Deputy Director of the UNU Geothermal Training Programme, for giving me the opportunity to participate in this special course. My sincere appreciation goes to my supervisors, Ms. Anette Mortensen, Dr. Hjalti Franzson, Dr. Björn S. Hardarson and Gudmundur Heidar Gudfinnsson for their guidance and sharing of their valuable knowledge. Many thanks go to Mr. Ingimar Gudni Haraldsson, Ms. Thórhildur Ísberg and Mr. Markús A.G. Wilde and all other UNU staff for their assistance, and coordination during my studies. I appreciate all lecturers from Orkustofnun and other institutions for giving their valuable input.

Special thanks go to my family for their support, encouragement and prayers during my stay in Iceland. The friends I made in Iceland are priceless to me and I appreciate all the support and encouragement they offered during the tough times. May God bless you all, abundantly.

Thank you, Almighty God, for the opportunities that you continue to offer me and the strength I needed in time of need. Glory be to You.

REFERENCES

Browne, P.R.L., 1984a: Subsurface stratigraphy and hydrothermal alteration of the Eastern section of the Olkaria geothermal field, Kenya. *Proceedings of the 6th New Zealand Geothermal Workshop, Geothermal Institute, Auckland,* 33-41.

Browne, P.R.L., 1984b: *Lectures in geothermal geology and petrology*. UNU-GTP, Iceland, report 2, 92 pp.

Dimitrios, G., 1989: *Magnetotelluric studies in geothermal areas in Greece and Kenya*. University of Edinburgh, PhD thesis, Edinburgh.

Furgerson, R.B., 1972: *Electrical resistivity survey of the Olkaria project, Kenya*. East African Power & Lighting Co., Ltd., UN Geothermal Exploration Project, report.

Kerr, P.F., 1977: *Optical mineralogy* (4th ed.). McGraw Hill, NY, 442 pp.

Lagat, J.K., 1998: *Borehole geology of well OW-801, Olkaria Southeast field*. KenGen, Kenya, internal report.

Lagat, J.K., 2004: *Geology, hydrothermal alteration and fluid inclusion studies of the Olkaria Domes geothermal field, Kenya.* University of Iceland, MSc thesis, UNU-GTP, Iceland, report 2, 71 pp.

MacKenzie, W.S., and Guilford, C., 1980: *Atlas of rock forming minerals in thin section*. Longman Group Ltd., London, 98 pp.

Mungania, J., 1992: *Preliminary field report on geology of Olkaria volcanic complex with emphasis on Domes area field investigations*. Kenya Power Company, Kenya, internal report.

Mungania J., 1999: *Summary of the updates of the geology of Olkaria Domes geothermal field*. KenGen, Kenya, internal report.

Mwangi, M.N., 1986: *Interpretation of additional sounding data at Olkaria, Kenya*. Kenya Power Company, Kenya, internal report.

Mwarania, F., 2010: *Completion tests report for well OW-911A*. KenGen, Kenya, internal report.
Naylor, W.I., 1972: *Geology of the Eburru and Olkaria prospects.* UN Geothermal Exploration Project, report.

Ndombi, J.M., 1981: The structure of the shallow crust beneath the Olkaria geothermal field, Kenya, deduced from gravity studies. *J. Volcanology and Geothermal Research, 9*, 237-251.

Njue, L.M., 2010: Borehole geology and hydrothermal mineralisation of well HE-27, Hellisheidi geothermal field, SW-Iceland. Report 24 in: *Geothermal training in Iceland 2010*. UNU-GTP, Iceland, 463-492.

Onacha, S.A., 1989: *An electrical resistivity study of the area between Mt. Suswa and the Olkaria geothermal field, Kenya*. University of Nairobi, MSc. thesis, Nairobi, 177 pp.

Onacha, S.A., 1990: *Olkaria West field information report*. Kenya Power Co., Kenya, internal report.

Onacha, S.A., 1993: *Resistivity studies of the Olkaria-Domes geothermal project.* Kenya Power Co., Kenya, internal report.

Omenda, P.A, 1998: The geology and structural controls of the Olkaria geothermal system, Kenya. *Geothermics, 27-1,* 55-74.

RockWare, 2007: *LogPlot program.* RockWare, Inc., USA.

Ryder, A.J.D., 1986: *Geological report of well OW-701 Olkaria geothermal field, Kenya.* Kenya Power Co., Kenya, report prepared by GENZL.

Saemundsson, K., and Gunnlaugsson, E., 2002: *Icelandic rocks and minerals*. Mál og menning, Reykjavík, Iceland, 233 pp.

Simiyu, S.M., and Keller, G.R., 1997: An integrated analysis of lithospheric structure across the East African plateau based on gravity anomalies and recent seismic studies. In: Fuchs, K., Altherr, R.,

Müller, B., and Prodehl, C. (eds.), *Structure and dynamic processes in the lithosphere of the Afro-Arabian rift system*. *Tectonophysics, 278,* 291-313.

Simiyu, S.M., and Malin, P.E., 2000: A "volcano seismic" approach to geothermal exploration and reservoir monitoring: Olkaria, Kenya and Casa Diablo, U.S.A. *Proceedings of the World Geothermal Congress 2000, Kyoto-Tohoku Japan*, 1759-1763.

Thomas, J., 2010: *Fairly simple geology exercises for students and their teachers.* Skidmore College, website: www.skidmore.edu.

APPENDIX I: Lithologic description and hydrothermal alteration minerals of drill cuttings of well OW-911A

The list of hydrothermal alteration minerals given for each rock type is based on binocular and petrographic microscopes and XRD analyses

Depth (m)	Description	Rock type	Alteration minerals
0-78	Light brown to grey lithic lava, has obsidian, pumice, and is vesicular with feldspar fillings	Pyroclasts	Clays
78-222	Circulation losses		
222-282	Dark grey, fine-grained porphyritic lava	Trachyte	Thomsonite
282-308	Light grey to light brown porphyritic lava. It is slightly oxidised from a depth of 306-308 m.	Rhyolite	Chlorite, hematite
308-356	Mixed fragments of brown, green, black and white. It is fine grained having altered glass with obsidian texture. At depth it becomes vesicular with phenocrysts.	Tuff	Chlorite, chalcedony,
356-432	There are two types of rhyolites at this range: the pantelleritic rhyolite occurs from 356-424 m; it is light grey to light brown fine-grained glassy rock. Amphibole occurs as dots in the matrix. At a depth of 424-432 m, the comenditic rhyolite appears as light green to grey aphanitic massive rock. It has obsidian texture.	Rhyolite	Chlorite, opal, quartz
432-496	Brownish grey fine-grained massive rock; it is moderately porphyritic with pyrite dissemination.	Trachyte	Agate, chalcedony, heulandite (468 m), chlorite, hematite
496-526	Brown to light green fine-grained vesicular rock with amygdules.	Tuff	Chalcedony, opal, quartz, hematite, chlorite
526-546	Greenish brown fine grained with flow texture and is vesicular.	Trachyte	Chlorite, chalcedony
546-600	Brown to green vesicular and is quite glassy. At 574-600 m it becomes more altered green clays with high calcite. It shows high permeability.	Tuff	Chlorite, quartz, brown clays
600-660	Light green to grey fine-grained vesicular bleached rock. It gets glassy and altered at a depth from 640-646 m, it has secondary quartz precipitate out, showing it's a vein or fracture zone.	Rhyolite	Chlorite, quartz, hematite, chalce-dony, agate, halcopyrite
660-664	Circulation losses.		
664-720	Light brown to grey fine-grained porphyritic rock. The groundmass is dotted with amphibole alteration. At a depth of 668 m, platy calcite was observed. This indicates boiling and that this is the depth at which the cap rock starts.	Rhyolite	Chlorite, epidote (670 m) prehnite (689 m), quartz
720-722	Circulation losses		
722-754	Greyish to pink crystalline massive rock with phenocrysts of sanidine. At 750 m platy calcite is still present.	Trachyte	Chlorite, prehnite
864-928	Light grey to light brown fine-grained crystalline rock.	Rhyolite	Chlorite, quartz, hematite, albite
928-940	Dark grey with white fragments. The groundmass is crystalline with phenocrysts.	Basalt	Prehnite, quartz
940-958	Dark grey with white fragments. The groundmass is crystalline with phenocrysts.	Trachyte	Epidote, chlorite, hematite, albite
958-964	Light grey to green, fine grounded porphyritic lava	Tuff	Epidote, quartz, chlorite

Depth (m)	Description	Rock type	Alteration minerals
964-970	Dark grey, fine-grained porphyritic lava. It is vesicular	Basalt	Epidote, prehnite, quartz, chlorite
970-978	Circulation losses		
978-1018	Green, crystalline porphyritic rock highly altered to green clays.	Basalt	Epidote, chlorite, quartz
1018-1050	Light grey, crystalline rock. At depth of 1042-1046, the rock becomes highly oxidized and altered to brown clay. Sequence is slightly porphyritic.	Rhyolite	Chlorite, epidote, albite, quartz
1050-1058	Light grey slightly altered to green clays, crystalline porphyritic lava. It is vesicular.	Tuff	Chlorite, quartz, epidote, albite
1058-1078	Greyish brown, fine-grained massive rock with flow texture.	Trachyte	Chlorite, brown clays
1078-1090	Green, crystalline porphyritic rock. It is highly altered to green clays.	Basalt	Epidote, chlorite, quartz
1090-1130	Brownish grey fine grained, sometimes porphyritic with pyroxene phenocrysts.	Trachyte	Chlorite, epidote, albite, quartz
1130-1156	Brown to light grey porphyritic rock.	Rhyolitic tuff	Quartz, chlorite, brown clays
1156-1162	Brown to light grey fine-grained massive rock.	Trachyte	Chlorite, brown clays
1162-1170	Green porphyritic rock.	Basalt	Chlorite, epidote, brown clays
1170-1176	Light grey to light green slightly porphyritic.	Rhyolite	Chlorite, brown clays
1176-1186	Brown to light grey porphyritic rock.	Trachyte	Albite, chlorite, quartz
1186-1192	Green porphyritic rock.	Basalt	Epidote, chlorite
1192-1234	Brown fine-grained massive rock. It is porphyritic with phenocrysts of albite.	Trachyte	Chlorite, albite, epidote, brown clays
1234-1242	Brown, porphyritic rock	Tuff	Chlorite, brown clays
1242-1246	Light grey to white porphyritic rock.	Rhyolite	Chlorite, yellow and brown clays, quartz
1246-1308	Grey, porphyritic rock with altered plagioclase phenocrysts.	Trachyte	Albite, hematite, brown clays
1308-1382	Light green to brown porphyritic rock.	Tuff	Epidote, brown and green clays, chlorite
1382-1388	Dark grey highly porphyritic rocks.	Basalt	Brown clays, sphene
1388-1436	Brown to dark grey highly porphyritic lava.	Tuff	Brown clays, chlorite, quartz, albite, blue clays
1436-1456	Greenish grey massive rock with phenocrysts.	Trachyte	Chlorite, quartz, albite
1456-1546	Brown massive fine-grained rock with porphyritic texture. It becomes more crystalline at a depth of 1508-1522 m.	Trachyte	Chlorite, epidote, brown and blue clays, albite, quartz
1546-1742	Dark grey to brown massive fine-grained porphyritic rock. It is also crystalline.	Trachyte	Albite, quartz, actinolite(1668 m), epidote, chlorite, brown and yellow clays
1742-1744	Loss of circulation		

Depth (m)	Description	Rock type	Alteration minerals
1744-1954	Brown to grey massive fine-grained crystalline rock. It has phenocrysts of alteration minerals. Rock changes to lighter grey more crystalline highly fractured at 1860-1906 m, with large actinolite growths. It is chloritized at 1924-1926 m.	Trachyte	Epidote, actinolite, wairakite, quartz, chlorite, wolla-stonite (1898 m), brown shiny clays
1954-1980	Dark grey crystalline porphyritic rock.	Basalt	Actinolite, quartz, epidote, wairakite
1980-2024	Grey massive fine grained slightly crystalline. It is highly fractured with sanidine phenocrysts.	Trachyte	Actinolite, quartz, wairakite, epidote, albite, brown clays
2024-2046	Greenish grey porphyritic rock, slightly crystalline rock	Crystalline tuff	Actinolite, quartz, chlorite, albite, brown clays
2046-2074	Grey crystalline highly fractured massive rock with sanidine phenocrysts.	Trachyte	Actinolite, wolla-stonite, epidote, quartz,chlorite,brown clays, wairakite
2074-2096	Grey to brown porphyritic rock.	Lithic tuff	Actinolite, epidote, albite, chlorite, brown clays
2096-2156	Green crystalline massive porphyritic rock. From 2120-2136 m It becomes brown fine-grained with mixed fragments.	Trachyte	Epidote, chlorite, prehnite
2156-2190	Light grey to brown crystalline rock.	Rhyolite	Brown clays, quartz, epidote, actinolite, wollastonite
2190-2238	Brown massive crystalline rock. It is porphyritic.	Trachyte	Actinolite, brown clays, albite, chlorite
2238-2246	Light brown to grey porphyritic rock.	Tuff	Shiny brown clays, actinolite, epidote
2246-2248	Dark grey fine-grained intrusive massive rock.	Basalt dyke	
2248-2292	Light brown to grey fragmented rock which is quite porphyritic.	Tuff	Actinolite, epidote, shiny brown clays, wollastonite, chlorite, quartz
2292-2294	Fine-grained massive rock, with light grey and dark grey fragments.	Basalt dyke	
2294-2316	Dark grey fragmented massive rock with feldspar phenocrysts.	Tuff	Actinolite, epidote, brown and green clays
2316-2318	Light grey and dark grey fine-grained massive fragment.	Basalt dyke	
2318-2352	Dark grey massive fragmented fine-grained rock. Abundant epidote possible feed zone at 2330-2338 m.	Tuff	Epidote, actinolite, wollastonite, brown clays
2352-2356	Dark grey fine-grained massive fresh rock. It has feldspar phenocrysts.	Basalt dyke	
2356-2370	Light grey massive fragmental rock. At 2364-2366 m, there are abundant actinolite and vein fillings. It is a possible feed zone.	Tuff	Chlorite, actinolite
2370-2376	Dark grey fine-grained massive fresh rock. It has feldspar phenocrysts.	Basalt dyke	
2376-2400	Dark grey to brown fine-grained massive fragmental rock. It has abundant actinolite as vein fillings at 2378-2380 m. It becomes more light grey and crystalline with abundant actinolite as vein fillings at 2394-2400 m	Tuff	Actinolite, chlorite, epidote

Depth (m)	Description	Rock type	Alteration minerals
2400-2410	Grey fine-grained massive slightly crystalline lava.	Trachyte	Actinolite
2410-2440	Light brown to grey fine-grained porphyritic fragmental rock. Feed zones are found at 2430-2432 m and 2436-2440 m, evidenced by abundant actinolite and epidote.	Tuff	Actinolite, chlorite, epidote, brown clays
2440-2496	Brown fine-grained massive rock. Alteration drastically increases at 2492-2494 m; it is a feed zone evidenced by abundant actinolite.	Trachyte	Actinolite, chlorite, brown clays
2496-2512	Green to dark grey highly altered rock. It is massive and has a porphyritic texture.	Basalt dyke	Actinolite, epidote, shiny brown clays
2512-2518	White to light grey sanidine phenocrysts with flow trachyitic texture coarse-grained rock.	Syenite dyke	Actinolite, epidote
2518-2530	White to light grey coarse-grained crystalline rock.	Rhyolite	Actinolite, quartz, epidote
2530-2558	Brown to grey fine-grained matrix, it is porphyritic with fragments. There is a feed zone at 2554-2556 m.	Tuff	Epidote, actinolite, brown clays
2558-2564	Shiny brown crystalline massive rock. It's a possible feed zone.	Trachyte	Epidote, shiny brown clays, acti-nolite
2564-2576	Green to dark grey highly altered porphyritic rock.	Basalt dyke	Actinolite, epidote
2576-2624	Brown to grey fine-grained massive rock. At depth between 2578-2580 alteration increases drastically and is a possible feed zone.	Trachyte	Actinolite, brown clays
2624-2626	Light grey to light brown crystalline rock.	Rhyolite	Actinolite, quartz, brown clays, chlorite, epidote
2626-2630	Green to dark grey highly altered porphyritic rock.	Basalt dyke	Actinolite, epidote
2630-2640	Light grey to light brown crystalline rock.	Rhyolite	Actinolite, quartz, brown clays, chlorite, epidote
2640-2670	Light grey to light brown crystalline rock.	Syenite dyke	Epidote, actinolite, chlorite, wolla-stonite, brown clays, quartz
2670-2700	Light grey to light brown crystalline rock. Abundant epidote between 2670-3674 m; it is a possible feed zone.	Trachyte	Epidote, actinolite, quartz, brown clays, chlorite
2700-2704	Dark green to dark grey fine-grained massive rock. It has a porphyritic texture.	Basalt dyke	Actinolite, epidote, quartz
2704-2724	Brownish grey fine-grained crystalline massive rock. A feed zone occurs at 2710-2714.	Trachyte	Actinolite, blue and brown shiny clays
2724-2740	Dark grey fine-grained massive rock. It is porphyritic. At 2738-2740 it becomes more altered to green clays and epidote.	Basalt	Actinolite, brown shiny clay, epidote
2740-2754	Grey fine-grained massive crystalline rock.	Trachyte	Actinolite, brown clays
2754-2756	Light grey crystalline coarse-grained rock with flow texture.	Syenite dyke	Actinolite
2756-2876	Light grey fine-grained massive rock. It becomes more altered with depth. Possible feed zones are 2770-2772, 2780-2782, 2856-2862, 2904-2906 and 296-2972 m. This is because of abundant epidote and actinolite occurring in vein fillings.	Trachyte	Actinolite
2876-2886	Loss of circulation		
2886-3000	Light grey fine-grained massive rock. It is highly altered and fractured.	Trachyte	Actinolite

APPENDIX II: XRD graph analyses of chlorite, illite and mixed-layer clay peaks

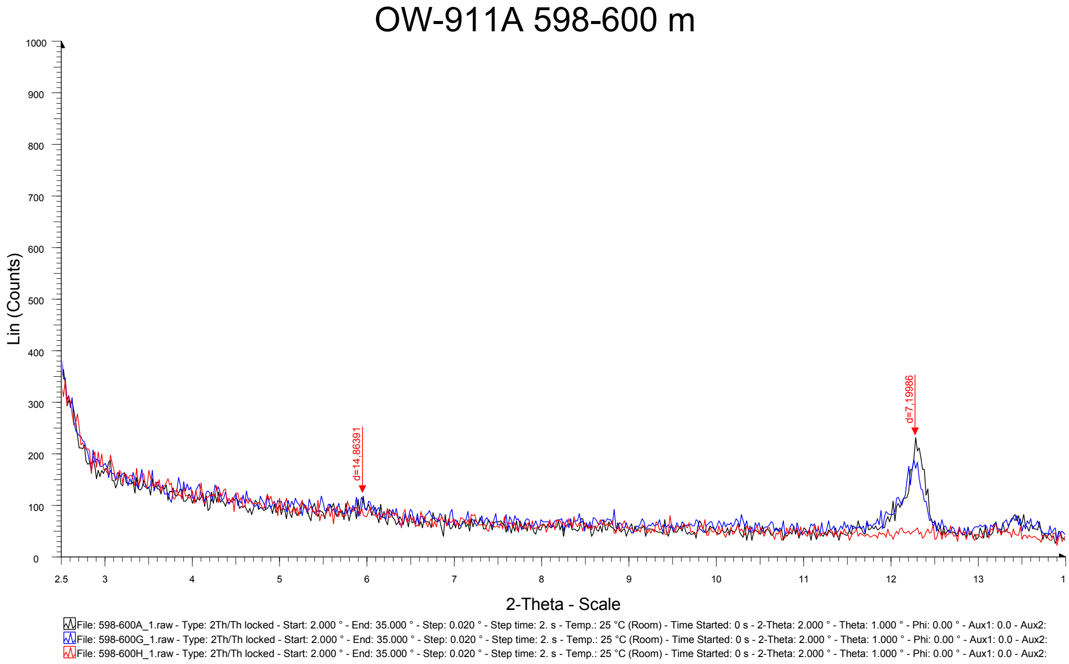

FIGURE 1: Diffractograms of clays showing strong chlorite peaks at around 7.19 and at 14.86 Å in the untreated, glycolated and the oven heated runs

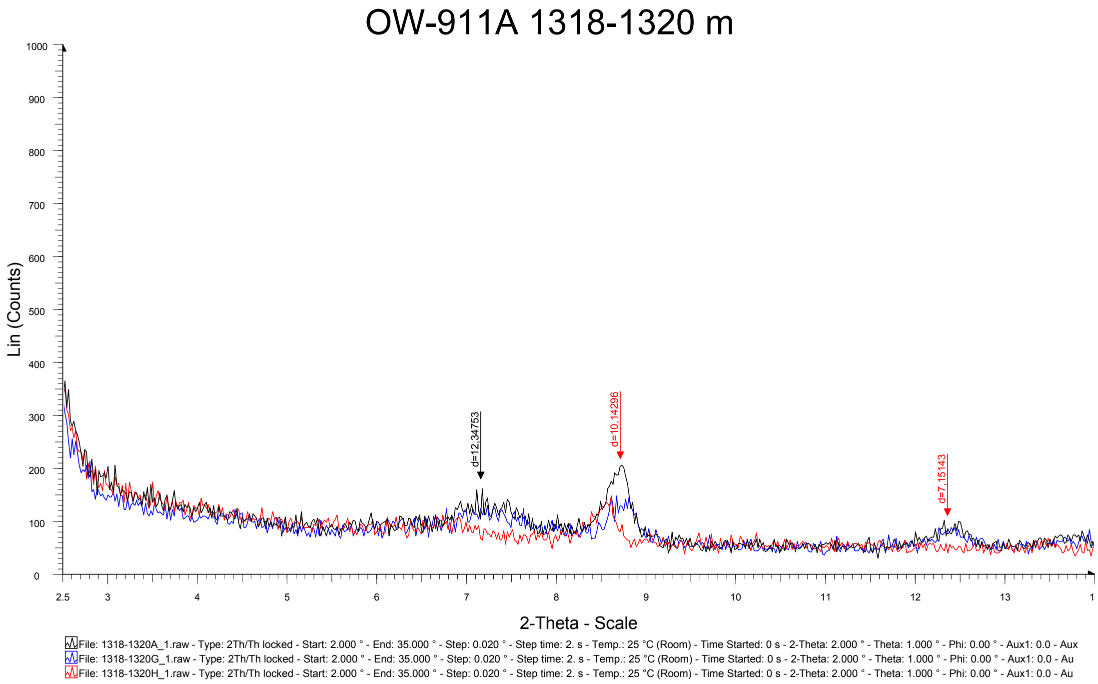

FIGURE 2: Diffractograms of clays showing strong illite peaks at around 10.14 Å and a minor chlorite component with peaks at 7.15 Å and mixed-layer clay at 12.34 Å
in the untreated, glycolated and the oven heated runs

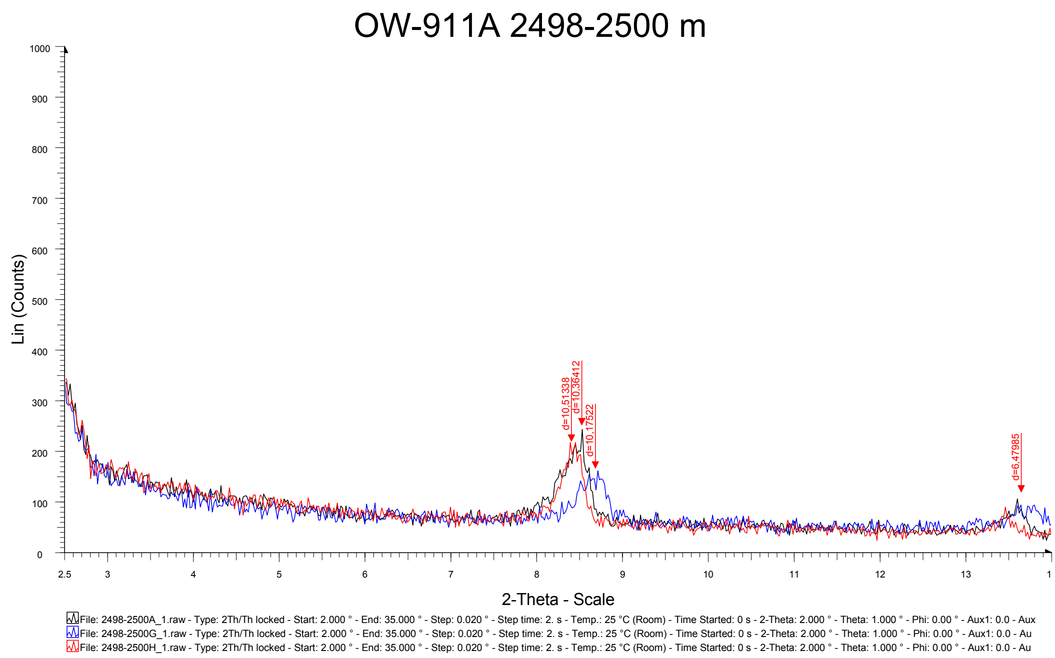

FIGURE 3: Diffractograms of clays showing strong illite peaks between 10.5 Å and 10.1Å and minor feldspar component with peaks at 6.47Å in the untreated, glycolated and the oven heated runs

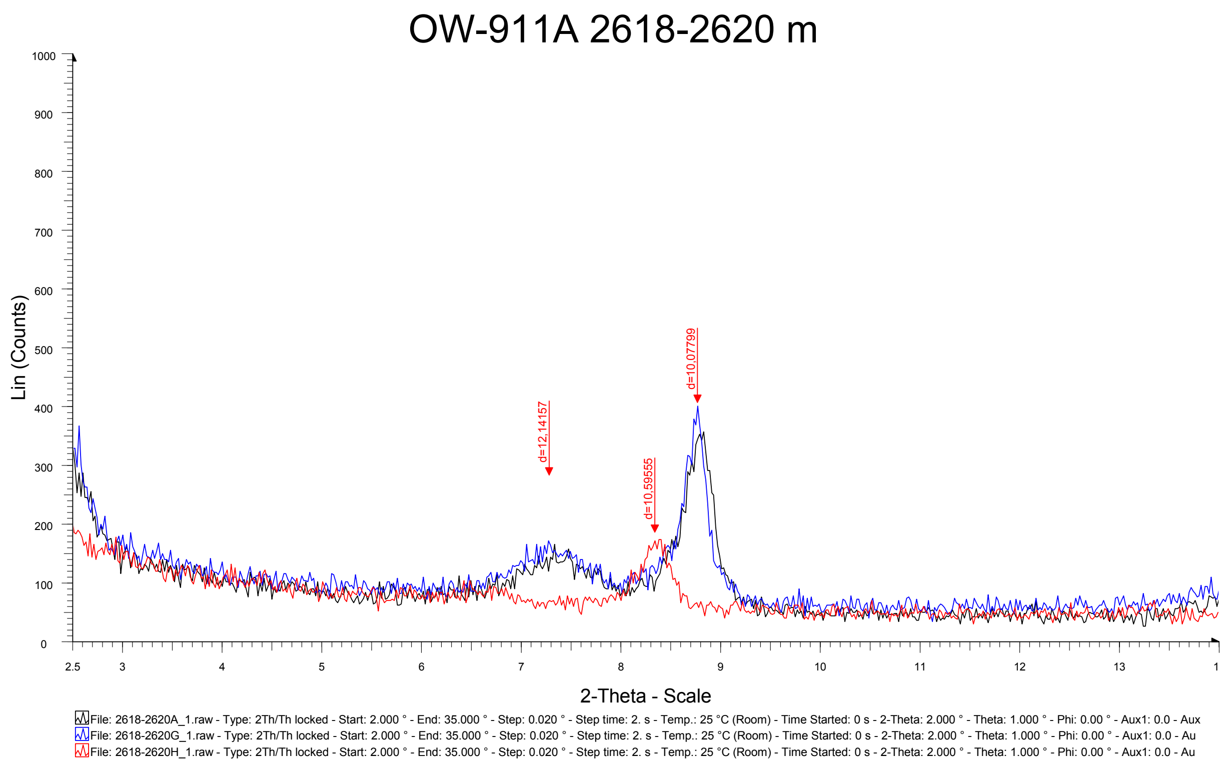

FIGURE 4: Diffractograms of clays showing strong illite peaks at around 10.58 and 10.07Å with minor mixed-layer clay with peaks at 12.14 Å in the untreated, glycolated and the oven heated runs